NASA/TM-20250003725

# Effect of Space Exposure on the Tensile Properties of MISSE Teflon Flight Samples

*Kim K. de Groh*
*Glenn Research Center, Cleveland, Ohio*

*Austin Whitt*
*HX5, LLC, Cleveland, Ohio*

*Bruce A. Banks*
*Science Applications International Corporation, Cleveland, Ohio*

April 2025

# NASA STI Program Report Series

Since its founding, NASA has been dedicated to the advancement of aeronautics and space science. The NASA scientific and technical information (STI) program plays a key part in helping NASA maintain this important role.

The NASA STI program operates under the auspices of the Agency Chief Information Officer. It collects, organizes, provides for archiving, and disseminates NASA's STI. The NASA STI program provides access to the NTRS Registered and its public interface, the NASA Technical Reports Server, thus providing one of the largest collections of aeronautical and space science STI in the world. Results are published in both non-NASA channels and by NASA in the NASA STI Report Series, which includes the following report types:

- TECHNICAL PUBLICATION.
  Reports of completed research or a major significant phase of research that present the results of NASA programs and include extensive data or theoretical analysis. Includes compilations of significant scientific and technical data and information deemed to be of continuing reference value. NASA counterpart of peer-reviewed formal professional papers but has less stringent limitations on manuscript length and extent of graphic presentations.

- TECHNICAL MEMORANDUM.
  Scientific and technical findings that are preliminary or of specialized interest, e.g., quick release reports, working papers, and bibliographies that contain minimal annotation. Does not contain extensive analysis.

- CONTRACTOR REPORT.
  Scientific and technical findings by NASA-sponsored contractors and grantees.

- CONFERENCE PUBLICATION.
  Collected papers from scientific and technical conferences, symposia, seminars, or other meetings sponsored or cosponsored by NASA.

- SPECIAL PUBLICATION.
  Scientific, technical, or historical information from NASA programs, projects, and missions, often concerned with subjects having substantial public interest.

- TECHNICAL TRANSLATION.
  English-language translations of foreign scientific and technical material pertinent to NASA's mission.

Specialized services also include organizing and publishing research results, distributing specialized research announcements and feeds, providing information desk and personal search support, and enabling data exchange services.

For more information about the NASA STI program, see the following:

- Access the NASA STI program home page at http://www.sti.nasa.gov

NASA/TM-20250003725

# Effect of Space Exposure on the Tensile Properties of MISSE Teflon Flight Samples

*Kim K. de Groh*
*Glenn Research Center, Cleveland, Ohio*

*Austin Whitt*
*HX5, LLC, Cleveland, Ohio*

*Bruce A. Banks*
*Science Applications International Corporation, Cleveland, Ohio*

National Aeronautics and
Space Administration

Glenn Research Center
Cleveland, Ohio 44135

April 2025

## Acknowledgments

We are grateful to the NASA Flight Opportunities program, the International Space Station Program Office and Aegis Aerospace for making these flight opportunities possible. We would also like to thank Diane Malarik of NASA Headquarters, along with Craig Robinson and Kelly Bailey of NASA Glenn Research Center for their long-term support of these MISSE-FF experiments. This work is supported by the Biological and Physical Sciences Division.



*Level of Review*: This material has been technically reviewed by technical management.

This report is available in electronic form at https://www.sti.nasa.gov/ and https://ntrs.nasa.gov/

NASA STI Program/Mail Stop 050
NASA Langley Research Center
Hampton, VA 23681-2199

# Contents

# Effect of Space Exposure on the Tensile Properties of MISSE Teflon Flight Samples

Kim K. de Groh
National Aeronautics and Space Administration
Glenn Research Center
Cleveland, Ohio 44135

Austin Whitt
HX5, LLC
Cleveland, Ohio 44135

Bruce A. Banks
Science Applications International Corporation
Cleveland, Ohio 44135

## Abstract

Materials on the exterior of spacecraft in low Earth orbit (LEO) are subject to extremely harsh environmental conditions including various forms of radiation, temperature extremes and thermal cycling, impacts from micrometeoroids and orbital debris, on-orbit contamination, and atomic oxygen (AO) exposure. Radiation combined with thermal exposure can cause embrittlement of thin film polymers, such as the Teflon fluorinated ethylene propylene (FEP) insulation on the exterior of the Hubble Space Telescope. To better understand the effect of space exposure on the mechanical property degradation of Teflon FEP and other thin film spacecraft polymers, 116 tensile samples were exposed to the space environment on the exterior of the International Space Station (ISS) and returned to Earth for mechanical testing. The samples were flown in either zenith or wake orientations as part of three Materials International Space Station Experiment (MISSE) mission experiments. These experiments are the Polymers Experiment with 30 zenith tensile samples flown as part of the MISSE-8 mission, the Polymers and Composites Experiment-1 (PCE-1) with 24 zenith and 38 wake tensile samples flown as part of the MISSE-9 mission, and the PCE-4 with 24 zenith samples flown as part of the MISSE-13 mission. Two of the MISSE-9 wake samples broke while on-orbit. Post-flight tensile testing was successfully completed on 114 flight and 116 control samples. All Teflon FEP samples were embrittled due to the space exposure. The zenith FEP samples were consistently more embrittled than the wake samples for the same exposure duration. The metallized Teflon samples were more embrittled than the clear Teflon samples for the same exposures. The slightly longer MISSE-9 wake exposure (0.54 years) caused more embrittlement of the Teflon FEP samples than the MISSE-13 wake exposure (0.44 years). A multi-layered stack of 2 mil Teflon FEP indicated that deeper penetrating radiation can cause embrittlement, but less penetrating radiation causes the majority of the damage. Teflon with a black carbon back-surface coating showed that a higher on-orbit temperature causes a synergistic effect that increases the radiation-induced embrittlement of Teflon FEP in LEO. In addition, metallized Polyimide Colorless (CP1) thin film solar sail materials had no significant embrittlement after 0.44 years of LEO wake exposure during the MISSE-13 mission.

# Introduction

Materials used on the exterior of spacecraft are subjected to many environmental threats that can cause degradation. In low Earth orbit (LEO) these threats include visible light photon radiation, ultraviolet (UV) radiation, vacuum ultraviolet (VUV) radiation, solar flare x-rays, solar wind particle radiation (electrons and protons), cosmic rays, temperature extremes and thermal cycling, impacts from micrometeoroids and orbital debris, on-orbit contamination, and atomic oxygen (AO). These environmental exposures can result in erosion, embrittlement and optical property degradation of susceptible materials which threatens spacecraft performance and durability.

Atomic oxygen is a particularly serious threat to the structural, thermal, and optical properties of oxidizable spacecraft components. Atomic oxygen is formed in the LEO environment through photodissociation of diatomic oxygen ($O_2$). In LEO, between the altitudes of 180 and 650 km, AO is the most abundant species.[1] Atomic oxygen can react with polymers, carbon, and many metals to form oxygen bonds with atoms on the exposed surface. For most polymers, hydrogen abstraction, oxygen addition, or oxygen insertion can occur, with the oxygen interaction pathways eventually leading to volatile oxidation products.[2,3] This results in erosion of hydrocarbon or halocarbon material, with the exception of silicone materials, which form a glassy silicate surface layer with AO exposure.[4] Solar radiation can result in bond breakage in materials such as polymers through chain scission, and can impact the erosion of some materials, adding to the effects of AO.[3]

Space radiation, including solar UV, solar flare x-ray, and charged particle radiation, can cause serious polymer embrittlement of spacecraft materials. For example, the metallized Teflon FEP multilayer insulation (MLI) blanket outer layer on the Hubble Space Telescope (HST) has become extremely embrittled in the space environment resulting in severe on-orbit through-thickness cracking. This became evident during the second servicing mission (SM2) after 6.8 years of space exposure where cracking of the 5 mil (127 μm) thick Al-FEP outer layer of the HST MLI blankets was observed on the Light Shield, forward shell, and equipment bays.[5,6] Figure 1 shows large cracks in the outer layer of the solar facing Light Shield MLI on the HST as observed during SM2 after 6.8 years of space exposure.[6] By the time of the fifth servicing mission (called SM4), there were hundreds of cracks in the Al-FEP outer layer of the HST MLI blankets.[7] Figure 2 shows extensive cracking of the MLI outer layer as observed during SM4 after 19 years of space exposure.[8,9] MLI blanket sections were retrieved during the SM4 mission and the Al-FEP outer layer from Bay 8, which received direct sunlight, was found to fracture like thin brittle glass.[7]

Figure 1. Large cracks in the outer layer of solar facing MLI on the HST as observed during SM2 after 6.8 years of space exposure.[6]

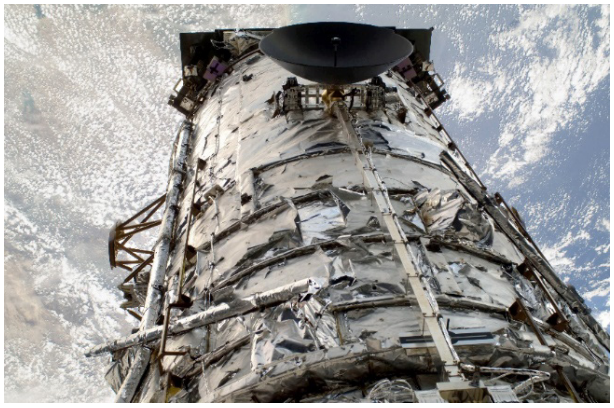

a.

b.

Figure 2. Severe cracking of the HST aluminized-Teflon outer layer of MLI after 19 years of space exposure. (a) Light Shield section with Earth in the background, and (b) Close-up image of the Light Shield MLI cracking.[8,9]

The spaceflight orientation highly affects the environmental exposure of spacecraft surfaces. Ram facing surfaces (facing the direction of travel) receive a high flux of directed AO (ram AO) and sweeping (moderate) solar exposure. Zenith facing surfaces (direction facing away from Earth) receive a low flux of grazing arrival AO and the highest solar exposure. Wake facing surfaces (facing away from the direction of travel) receive essentially no AO flux and moderate solar radiation (levels similar to ram experiments). Finally, nadir facing surfaces (direction facing towards Earth) receive a low flux of grazing arrival AO and minimal solar radiation (albedo sunlight). All surfaces receive charged particle and cosmic radiation, which are omnidirectional. Figure 3 provides a diagram of the ram, wake, zenith, and nadir flight orientations on the International Space Station (ISS). It should be noted that the actual orientation of the ISS varies due to operational requirements with the majority of the time spent within ±15 degrees of the +XVV Z nadir flight attitude (X Axis Near Velocity Vector, Z Axis Nadir/Down). Deviations from this attitude to accommodate visiting spacecraft, and other ISS operational needs, can cause variations in the orientation directions, and hence variations in environmental exposures especially for AO exposure of zenith and nadir surfaces.

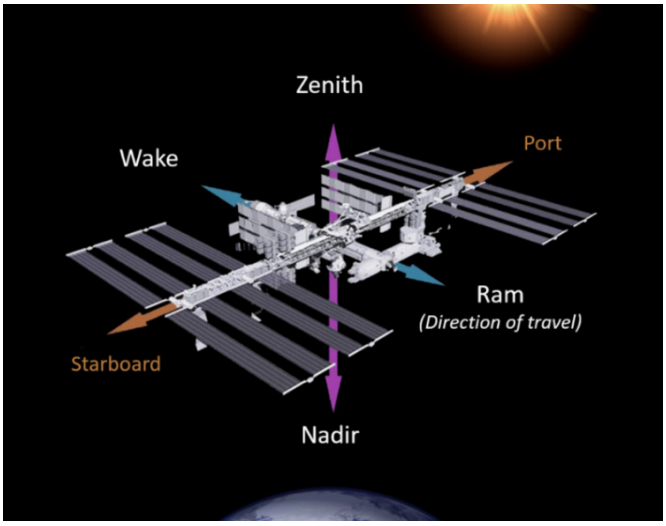


Figure 3. Diagram showing ram, wake, zenith, and nadir directions on the ISS.

Since 2001, NASA Glenn Research Center has flown a series of space exposure experiments as part of the Materials International Space Station Experiment (MISSE) missions on the exterior of the ISS.[10-18] Although Glenn's MISSE experiments have a variety of objectives, many of the 40+ experiments were flown to increase our understanding of AO erosion and radiation induced embrittlement of spacecraft thin film polymers.[10-18]

Teflon FEP tensile samples were flown as part of three NASA Glenn Research Center Materials International Space Station Experiment-7 (MISSE-7) experiments that were exposed to the space environment on the exterior of the ISS for 1.5 years.[17] Including Teflon tensile samples in each of the three experiments enabled similar samples to be exposed to ram, wake, zenith, and nadir orientations for the same mission duration. Nineteen total samples were flown, including Al-FEP in every flight orientation, carbon back-surface painted FEP (C-FEP, also called FEP/C) in the ram orientation and expanded-polytetrafluoroethylene (ePFTE) in the zenith orientation.[17] Tensile properties were obtained for 16 flight samples (three C-FEP samples cracked while on-

orbit). The results showed that prolonged exposure to the space environment can cause catastrophic degradation of 2 mil Al-FEP, a commonly used spacecraft thermal control material. The extent of degradation was found to be dependent on exposure orientation. Exposure in a nadir orientation caused minimal damage (average of 4% decrease in elongation).[17] Exposure in a wake orientation resulted in embrittlement (average of 44% decrease in elongation).[17] Exposure in a ram orientation caused large thickness loss and significant embrittlement (average of 71% decrease in elongation).[17] Exposure in a zenith orientation resulted in extensive embrittlement of 2 mil Al-FEP (average of 76% decrease in elongation).[17] The MISSE-7 tensile data indicated that solar radiation, and the associated heating, was the primary driver of embrittlement of FEP in the space environment, consistent with prior HST Teflon FEP analyses. Data supporting this was on-orbit cracking of carbon back-surface coated samples, which provided evidence that temperature plays a key role in augmenting the radiation-induced degradation of FEP.

To provide additional understanding of the effect of space exposure on the mechanical property degradation of Teflon FEP insulation and other thin film spacecraft polymers, 116 tensile samples were flown in zenith or wake orientations as part of three more recent NASA Glenn Research Center MISSE experiments: 1) The Polymers Experiment with 30 zenith tensile samples flown as part of the MISSE-8 mission, 2) The Polymers and Composites Experiment-1 (PCE-1) with 24 zenith and 38 wake tensile samples flown as part of the MISSE-9 mission, and 3) The PCE-4 with 24 wake samples flown as part of the MISSE-13 mission.[13,18] The samples included two thicknesses of Teflon FEP (2 and 5 mil thick) and Teflon FEP with various back-surface coatings (aluminum (Al), silver/Inconel (Ag/Inconel) and carbon paint to provide passive on-orbit heating). In addition, CP1 (clear polyimide) samples were flown on MISSE-8 and gossamer thin solar sail material samples were flown on MISSE-13. The samples were tensile tested post-flight. This paper provides an overview of the MISSE missions, the MISSE flight experiments, details on the tensile samples, the flight mission exposure data, and the post-flight tensile results.

## Materials International Space Station Experiment (MISSE) Missions

### *Materials International Space Station Experiment 1-8 (MISSE 1-8)*

In the MISSE 1–8 missions, individual flight experiments were flown in suitcase-like containers called Passive Experiment Containers (PECs) that provided exposure to the space environment. The PECs were placed outside the ISS in various locations by an astronaut during an extravehicular activity (EVA), or spacewalk. The PECs were positioned in either a ram/wake or a zenith/nadir orientation and exposed for 1-4 years between August 2001 and July 2013.[10,11] After the mission exposure, the PECs were retrieved during an EVA, and returned on the shuttle for post-flight analyses. The exception was MISSE-8 which was returned as part of the SpaceX-3 mission in July 2013.

### *Materials International Space Station Experiment-Flight Facility (MISSE-FF)*

In the post-shuttle Era, MISSE missions are flown on the MISSE-Flight Facility (MISSE-FF), ISS's permanent external material science platform. The MISSE-FF is operated by Aegis Aerospace (formerly Alpha Space Test & Research Alliance, LLC).[19] It is a modular and robotically serviceable external facility that is located on ISS Express Logistics Carrier-2 Site 3 (ELC-2 Site 3). It provides ram, wake, zenith, and nadir exposures. The MISSE-FF supports both passive and active experiments, with downlink of data. On-orbit facility cameras are scheduled to provide monthly sample images.

MISSE Sample Carriers (MSCs), also called MISSE Science Carriers, house the material flight experiments. Each MSC has two sides, a mount-side (MS) and a swing-side (SS), with a central hinge. Materials and spacecraft components can be flown on either the MS or SS decks for direct space exposure, or they can be mounted on the underdecks. The MSCs are launched closed as pressurized cargo on either the Northrup Grumman Cygnus or SpaceX Dragon spacecraft, moved outside the ISS through the Kibo Japanese Experiment Module (JEM) Airlock on the MISSE Transfer Tray (MTT), then installed on the MISSE-FF structure via robotic arm. The SS decks are remotely opened to expose the experiments to space. The MSCs are closed during resupply ship dockings to prevent contamination and ISS orientation changes to minimize AO exposure of wake surfaces. The MSCs are typically closed during local EVAs and for on-demand images.

The MSCs get initial space vacuum exposure when the JEM airlock is put under vacuum and opened to space. It can take several days to robotically move the MTT with the MSCs to ELC-2 and install the MSCs in the MISSE-FF. Each MSC is then remotely "deployed" or opened to the space environment for the first time. As mentioned above, the MSCs are typically closed and re-opened numerous times during a mission. The MSCs are then closed for a final time, robotically retrieved from the MISSE-FF and placed back into the MTT, and the MTT is robotically moved back into the JEM airlock and re-pressurized. Thus, the space vacuum exposure is longest, then the duration installed on the MISSE-FF, then the "deployed duration" (first time opened to final time closed), and finally the time directly exposed to space (accumulated open durations).

The MISSE-FF and the inaugural set of experiments, called MISSE-9, were launched aboard the SpaceX Commercial Resupply Services-14 (CRS-14) Dragon, also called SpaceX-14, on April 2, 2018. The MISSE-FF was robotically installed on ELC-2 Site 3 on April 8, 2018. The MISSE-9 MSCs were installed in the MISSE-FF on April 18-19, 2018. The MISSE-9 PCE-1 samples (flown in ram R2 MSC 3, wake W3 MSC 8 and zenith Z3 MSC 5) were deployed on April 19, 2018 and scheduled for a 1-year space exposure mission. Figure 4 provides an image showing the location of the MISSE-FF on ELC-2. Figure 5 provides an image of the wake side of the MISSE-FF with the one of the MSCs opened.

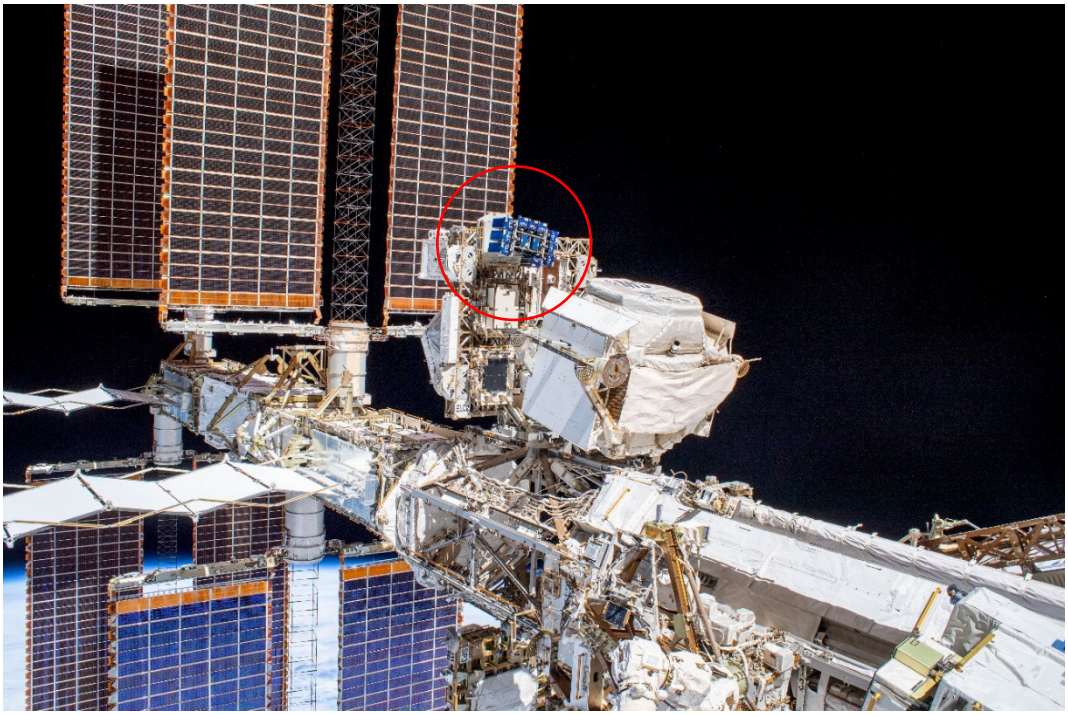

Figure 4. A view of the MISSE-FF on ELC-2 Site 3 as photographed during an EVA on November 15, 2019 (iss061e040917).

Figure 5. The wake side of the MISSE-FF with the central wake MSC open as photographed on January 25, 2020 during an EVA (iss061e143021).

## MISSE Flight Experiments

### *MISSE-8 Polymers Experiment*

The MISSE-8 mission consisted of a PEC and a smaller passive tray called the Optical Reflector Materials Experiment III (ORMatE-III). The PEC was attached to the exterior of the ISS on the EXPRESS Logistics Carrier 2 (ELC 2) in a zenith/nadir orientation during an extravehicular activity as part of the STS-134 Shuttle mission on May 20, 2011. Because of concerns of outgas contamination from the neighboring Alpha Magnetic Spectrometer (AMS) payload, ORMatE-III was deployed in a ram/wake orientation during the STS-135 Shuttle mission on July 12, 2011, approximately two months after deploy of the MISSE-8 PEC. Once positioned on ELC 2, the PEC and ORMatE-III remained exposed to the LEO space until they were retrieved on July 9, 2013 after 2.14, and 2.00 years of space exposure, respectively, and returned to Earth in the SpaceX-3 Dragon. Figure 6 shows the location of the MISSE-8 PEC and ORMatE-III on the ISS ELC-2. Figure 7 shows an on-orbit image of the MISSE-8 zenith/nadir PEC as imaged during the STS-135 ORMatE-III deploy mission in July 2011.

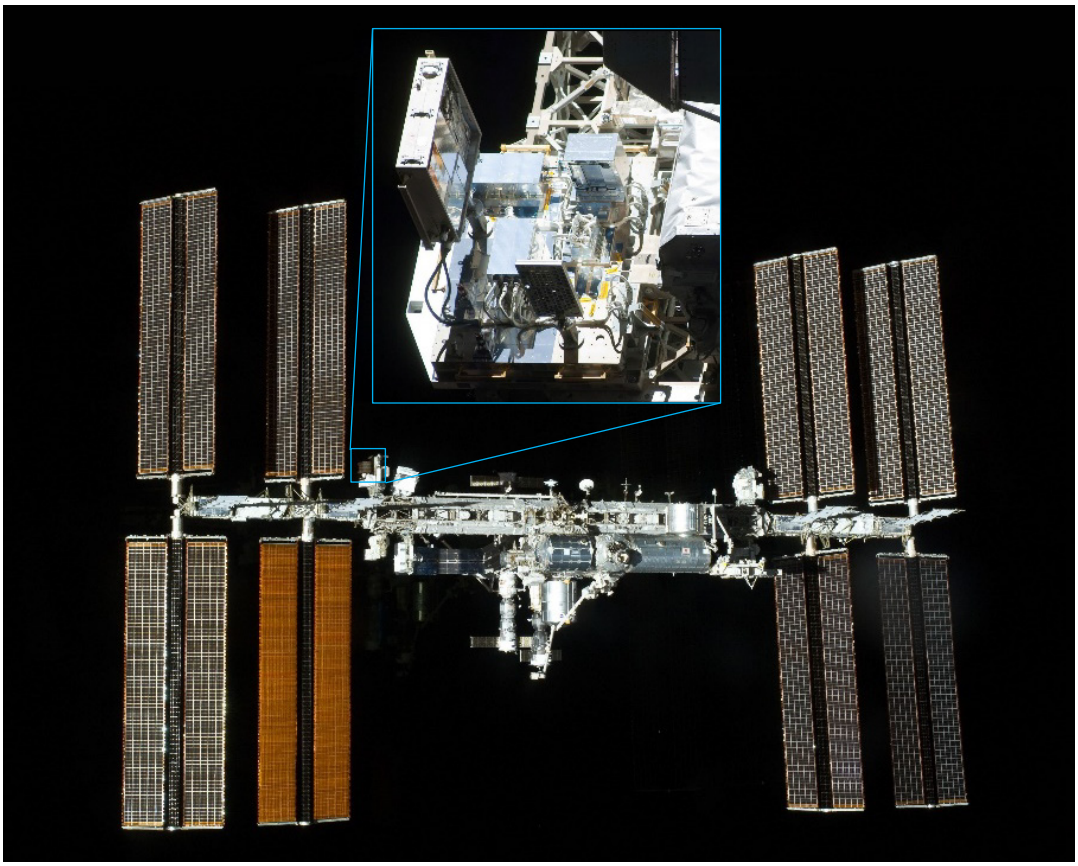

Figure 6. Location of MISSE-8 PEC and ORMatE-III on the ISS ELC-2 as imaged during the STS-135 shuttle mission in July 2011 shortly after deployment of ORMatE-III.

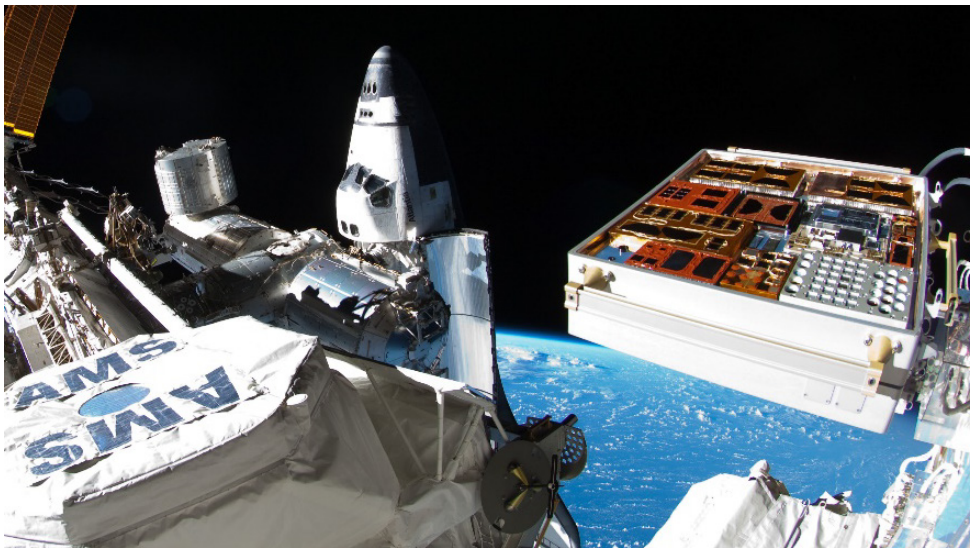

Figure 7. An on-orbit image of the MISSE 8 zenith/nadir PEC as imaged during the STS-135 ORMatE-III deploy mission in July 2011. The zenith face is visible.

The MISSE-8 Polymers Experiment was a passive experiment that included 42 samples, which were flown in ram (8 samples), wake (11 samples) or zenith (36 samples) orientations.[13] The primary objective of the Polymers Experiment was to determine the effect of solar exposure on the AO erosion yield ($E_y$) of fluoropolymers. The $E_y$ is the volume of material that is removed (through oxidation) per incident oxygen atom and is measured in units of $cm^3$/atom. The MISSE-8 Polymers Experiment also included a variety of other samples including Kapton H for AO fluence determination in each flight direction and tensile samples for space embrittlement assessment. Details and results on the AO $E_y$ samples are provided by de Groh in reference 13.

A total of 12 tensile samples were flown in the zenith direction along with a sample (M8-6) consisting of a set of six stacked rectangular pieces (1.5" (3.8 cm) x 2.6" (6.6 cm)) of Teflon FEP. Three tensile samples could be cut from each of the six stacked FEP layers post-flight for a total of 18 tensile samples. Thus, a total of 30 zenith tensile samples were flown as part of the MISSE-8 Polymers Experiment. Table 1 provides a list of the MISSE-8 Polymers Experiment zenith tensile samples along with the sample ID, material, abbreviation, thicknesses and number of flight and control samples. The majority of samples were 2 mil-thick (50.8 μm). The manufacturer and material lot number for the flight sample material is provided in Table A-1 of the Appendix. Older batch Teflon FEP materials were used so that the tensile data could be compared to prior flight and ground-test data for the same batch of material. For example, the 2 mil Al-FEP (M8-7) from Sheldahl lot #502532-2 was also used for the MISSE-7 tensile samples discussed in reference 17.

Flight and control tensile samples were punched from the film sheets using a die fabricated to the specifications defined in the American Society for Testing and Materials (ASTM) Standard D-638 for Type-V tensile specimens.[20] The tensile samples and stacked FEP sample were mounted in handmade thin Al foil holders which were taped in place to the MISSE-8 zenith deck using thermal control insulation tape. The entire neck region and a large portion of the grip region of the tensile samples were exposed to the LEO space environment. A pre-flight photograph of the zenith side of MISSE-8 is shown in Figure 8 with a close-up photograph of the zenith taped samples along with the sample IDs.

Table 1. MISSE-8 Polymers Experiment Zenith Tensile Samples.

| GRC Sample ID | Material | Abbrev. | Nominal Thickness (mil) | # Flight Samples | # Control Samples |
|---|---|---|---|---|---|
| M8-6 | Multilayer Teflon FEP sheets (6 - 1.5" x 2.6" layers) | FEP | 2 | | 7* |
| | *Layer #1 – Top space-exposed layer* | | | 3 | |
| | *Layer #2* | | | 3 | |
| | *Layer #3* | | | 3 | |
| | *Layer #4* | | | 3 | |
| | *Layer #5* | | | 3 | |
| | *Layer #6 – Bottom layer* | | | 3 | |
| M8-7 | Aluminized-Teflon FEP | Al-FEP | 2 | 3 | 6 |
| M8-8 | Carbon back-surface coated Teflon FEP | C-FEP | 2 | 3 | 3 |
| M8-9 | CP1 polyimide | CP1 | 1.07 | 3 | 6 |
| M8-11 | Teflon FEP | FEP | 2 | 3 | *M8-6 Controls |

In order to study the effect of on-orbit passive heating on the degradation of Teflon FEP tensile properties in LEO, three clear 2 mil (50.8 μm) thick Teflon FEP samples were coated on the back-surface with carbon paint (C-FEP) and flown as part of the MISSE-8 Polymers Experiment. These samples were flown because the C-FEP samples reach a higher on-orbit temperature than the Al-FEP samples of the same thickness due to their higher solar absorptivity. Maximum on-orbit temperature estimates were made based on solar absorptance and thermal emittance values for 2 mil Al-FEP and C-FEP flown in the zenith orientation on MISSE 8.[13] The maximum estimated on-orbit temperature for Al-FEP was 2 °C, while the maximum estimated on-orbit temperature was estimated to be significantly higher for the C-FEP at 170 °C.[13] The C-FEP samples (M8-8) were prepared by AO treating the non-exposed side of a clear FEP film to increase adherence prior to coating the surface with a layer of carbon paint. It should be noted that the C-FEP samples are abbreviated as FEP/C in reference 13. The stacked sample (M8-6) was flown to assess the embrittlement versus the depth of a multilayered sample. Thin film (1.07 mil thick) LaRC™ CP1 (CP1) from SRS Technologies was also flown.

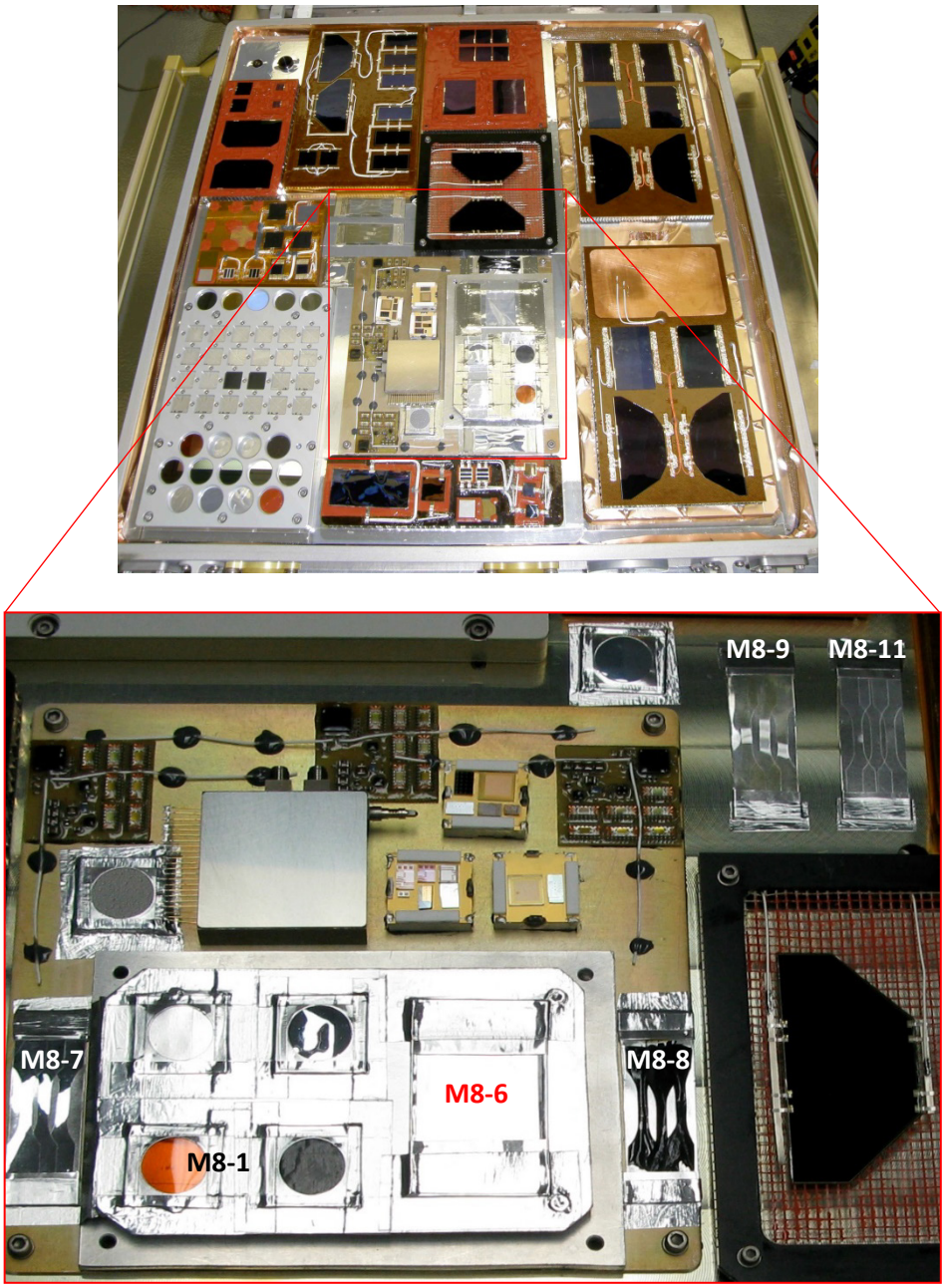


Figure 8. Pre-flight image of the zenith side of the MISSE 8 PEC with a close-up of the taped samples section (rotated) and with the Polymers Experiment samples identified. *(Photo credit: Naval Research Laboratory)*

### *MISSE-9 Polymers and Composites Experiment-1 (PCE-1)*

The Polymers and Composites Experiment-1 (PCE-1) was flown as part of the MISSE-9 inaugural mission of MISSE-FF. The MISSE-9 PCE-1 is a passive experiment with 138 samples that were flown in ram (39 samples), wake (52 samples) and zenith (47 samples) orientations. The primary objective of the PCE-1 is to determine the LEO AO $E_y$ of spacecraft polymers, composites,

and coated samples as a function of solar irradiation and AO fluence. Samples were also included to determine the mission AO fluence and on-orbit molecular contamination each flight direction. In addition, thin film polymer tensile samples were flown in the wake and zenith directions for studying space radiation induced embrittlement. A complete list of the PCE-1 samples is provided by de Groh in Reference 18 along with additional experiment objectives and pre-flight photos of select PCE-1 experiment samples.

Figure 9 shows a pre-flight photograph of the MISSE-9 PCE-1 samples loaded into the MISSE Sample Carrier (MSC) ram, wake and zenith flight mount-side (MS) decks. Each deck includes samples from two experiments, the PCE-1 and NASA Langley Research Center's Polymeric Materials Experiment. Figure 10 shows pre-flight photographs of the MISSE-9 decks with the PCE-1 samples outlined in red. The blank tensile holder "bars" shown in Figures 9 and 10 were replaced with bars that include sample numbers prior to flight, so that the tensile sample ID could be seen in the on-orbit images. Figure 11 shows photographs of the zenith (Figure 11a) and wake (Figure 11b) tensile samples mounted on the decks with the tensile ID bars. Figure 12 provides sample maps with the tensile sample IDs.

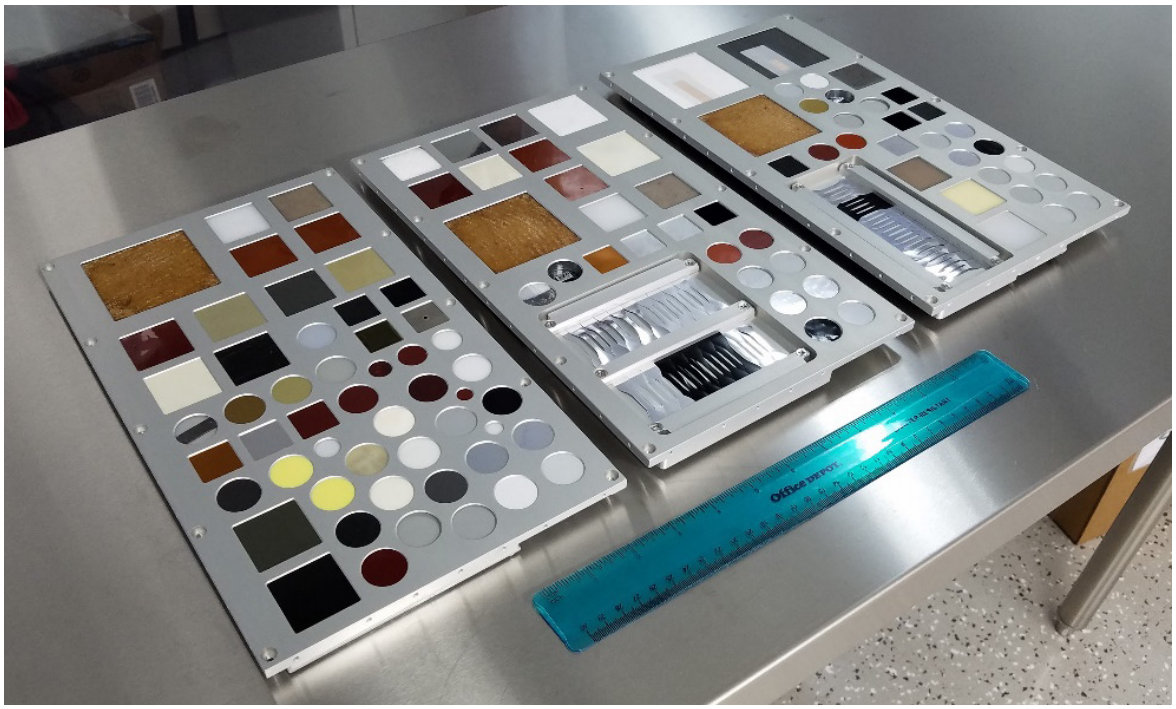


Figure 9. Pre-flight photograph of the MISSE-9 PCE-1 samples loaded into the MSC MS flight decks, from left to right: R2 MSC 3 (ram), W3 MSC 8 (wake), and Z3 MSC 5 (zenith).

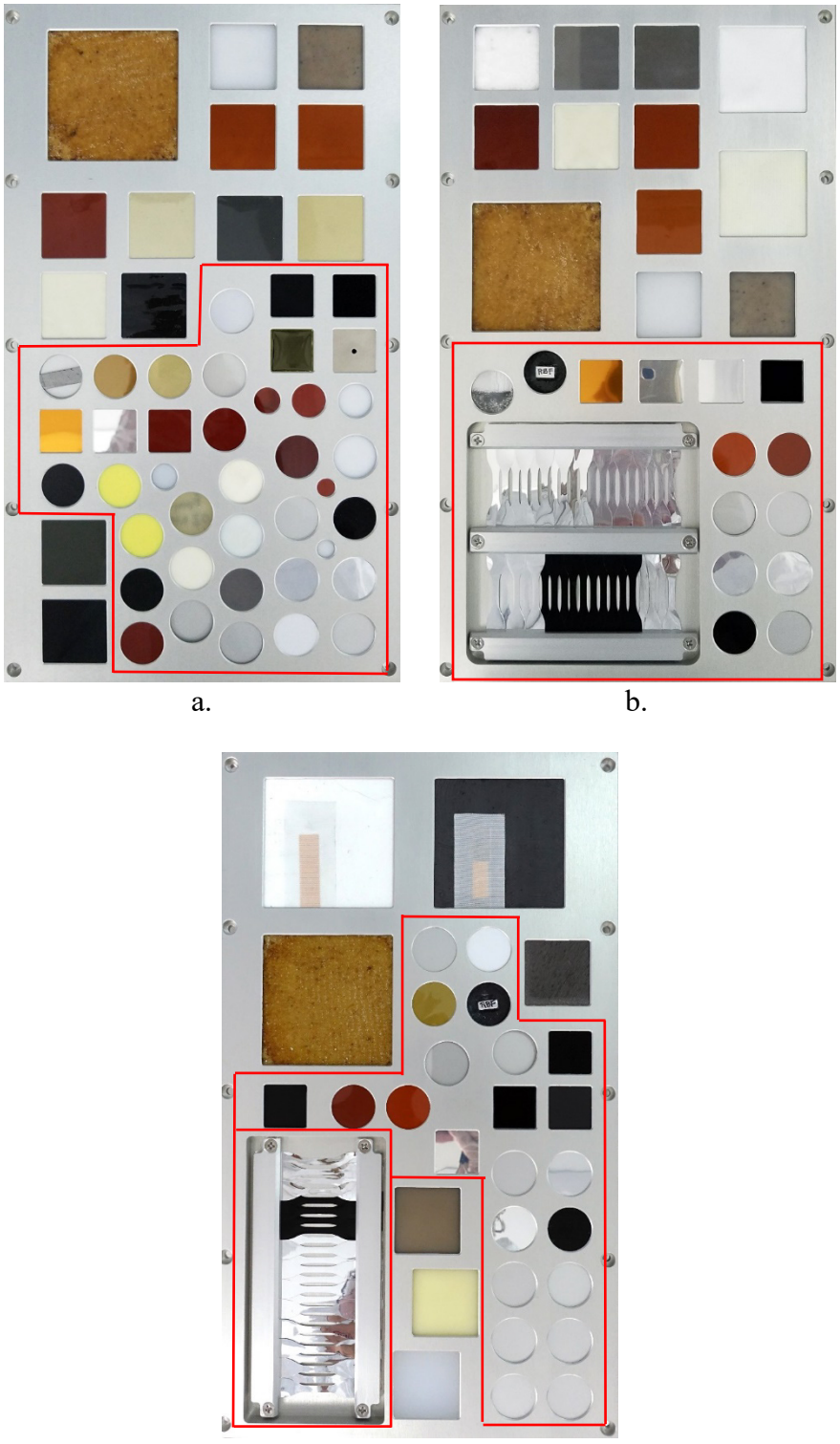

Figure 10. Pre-flight photographs of the MISSE-9 MSC decks with the PCE-1 samples outlined in red. (a). Ram samples in the R2 MSC 3 MS deck, (b) Wake samples in the W3 MSC 8 MS deck, and (c) Zenith samples in the Z3 MSC 5 MS deck.


a.


b.

Figure 11. Pre-flight photographs of the MISSE-9 tensile samples: a). Wake samples with ID#s 1-38, and b). Zenith samples with ID#s 1-24.*(Photo credit: Aegis Aerospace)*

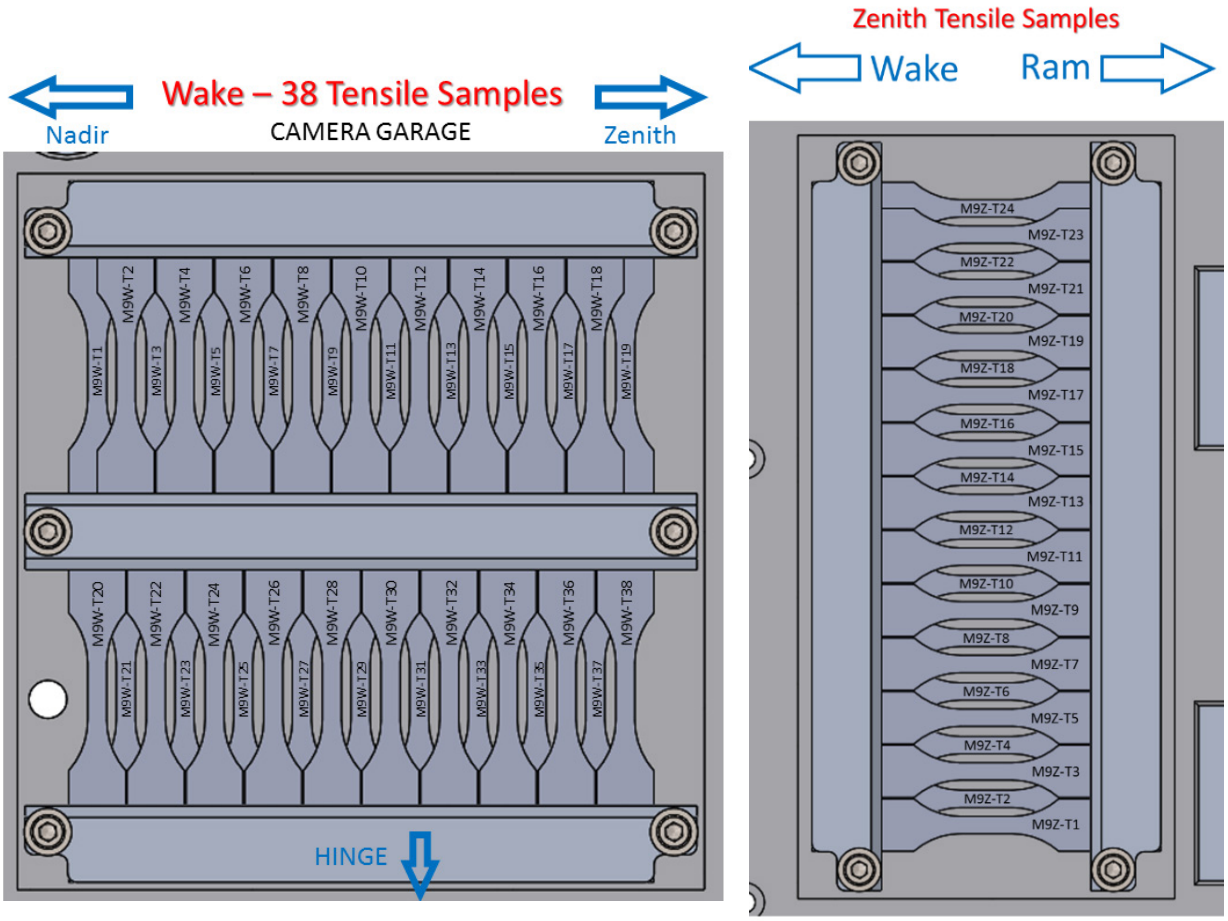


a. b.

Figure 12. Sample maps of the MISSE-9 tensile samples: a). Wake samples with ID#s 1-38, and b). Zenith samples with ID#s 1-24.

A total of 38 wake and 24 zenith flight tensile samples were flown as part of the PCE-1. Tables 2 and 3 provide lists of the MISSE-9 PCE-1 wake tensile and zenith tensile samples, respectively. These tables provide the MISSE-9 sample identification (ID), material, material abbreviation and film thickness. Like the MISSE-8 tensile samples, the flight and control tensile samples were punched from film sheets using a die fabricated to the specifications defined in the ASTM Standard D-638 for Type-V tensile specimens.[20] All the metallized film was purchased from Sheldahl. All the 2 mil Al-FEP was from the same batch of film (Sheldahl #502532-2) as the MISSE-8 Al-FEP. The manufacturer and material lot number for the flight sample material is provided in Table A-2 of the Appendix. All MISSE-9 flight samples were heated at 60 ºC for 24 hours under vacuum as part of Aegis Aerospace's flight hardware pre-flight testing. The control samples were not thermal vacuum exposed.

During hand delivery of the PCE-1 flight and back-up samples to Aegis Aerospace in Houston, TX for flight hardware integration, and post-flight for return of the flight samples to Cleveland, OH, arrangements were made for the samples to be exempt from airport x-ray screening to avoid non-space x-ray exposure. The back-up (control) samples were stored at NASA Glenn Research Center at ambient conditions (i.e. room temperature, 1 atm, etc.).

Table 2. MISSE-9 PCE-1 Wake Tensile Samples.

| MISSE-9 ID | Material | Parallel or Normal to Roll Lines | Abbreviation | Nominal Thickness (mils) | # Flight (F) Samples | # Control (C) Samples |
|---|---|---|---|---|---|---|
| M9W-T1 | Aluminized-Teflon | Parallel | Al-FEP (P) | 2 | | |
| M9W-T2 | Aluminized-Teflon | Parallel | Al-FEP (P) | 2 | | |
| M9W-T3 | Aluminized-Teflon | Parallel | Al-FEP (P) | 2 | 5 | 5 |
| M9W-T4 | Aluminized-Teflon | Parallel | Al-FEP (P) | 2 | | |
| M9W-T5 | Aluminized-Teflon | Parallel | Al-FEP (P) | 2 | | |
| M9W-T6 | Aluminized-Teflon | Normal | Al-FEP (N) | 2 | | |
| M9W-T7 | Aluminized-Teflon | Normal | Al-FEP (N) | 2 | | |
| M9W-T8 | Aluminized-Teflon | Normal | Al-FEP (N) | 2 | 5 | 5 |
| M9W-T9 | Aluminized-Teflon | Normal | Al-FEP (N) | 2 | | |
| M9W-T10 | Aluminized-Teflon | Normal | Al-FEP (N) | 2 | | |
| M9W-T11 | Aluminized-Teflon | Parallel | Al-FEP (P) | 5 | | |
| M9W-T12 | Aluminized-Teflon | Parallel | Al-FEP (P) | 5 | | |
| M9W-T13 | Aluminized-Teflon | Parallel | Al-FEP (P) | 5 | 5 | 4 |
| M9W-T14 | Aluminized-Teflon | Parallel | Al-FEP (P) | 5 | | |
| M9W-T15 | Aluminized-Teflon | Parallel | Al-FEP (P) | 5 | | |
| M9W-T16 | Aluminized-Teflon | Normal | Al-FEP (N) | 5 | | |
| M9W-T17 | Aluminized-Teflon | Normal | Al-FEP (N) | 5 | | |
| M9W-T18 | Aluminized-Teflon | Normal | Al-FEP (N) | 5 | 5 | 4 |
| M9W-T19 | Aluminized-Teflon | Normal | Al-FEP (N) | 5 | | |
| M9W-T20 | Aluminized-Teflon | Normal | Al-FEP (N) | 5 | | |
| M9W-T21 | Silver-Teflon^ | Parallel | Ag-FEP (P) | 5 | | |
| M9W-T22 | Silver-Teflon^ | Parallel | Ag-FEP (P) | 5 | 4 | 5 |
| M9W-T23 | Silver-Teflon^ | Parallel | Ag-FEP (P) | 5 | | |
| M9W-T24 | Silver-Teflon^ | Parallel | Ag-FEP (P) | 5 | | |
| M9W-T25 | Carbon painted (India Ink) Teflon | Parallel | C-FEP (P) | 2 | | |
| M9W-T26 | Carbon painted (India Ink) Teflon | Parallel | C-FEP (P) | 2 | | |
| M9W-T27 | Carbon painted (India Ink) Teflon | Parallel | C-FEP (P) | 2 | 5 | 5 |
| M9W-T28 | Carbon painted (India Ink) Teflon | Parallel | C-FEP (P) | 2 | | |
| M9W-T29 | Carbon painted (India Ink) Teflon | Parallel | C-FEP (P) | 2 | | |
| M9W-T30 | Carbon painted (India Ink) Teflon | Parallel | C-FEP (P) | 5 | | |
| M9W-T31 | Carbon painted (India Ink) Teflon | Parallel | C-FEP (P) | 5 | | |
| M9W-T32 | Carbon painted (India Ink) Teflon | Parallel | C-FEP (P) | 5 | 5 | 5 |
| M9W-T33 | Carbon painted (India Ink) Teflon | Parallel | C-FEP (P) | 5 | | |
| M9W-T34 | Carbon painted (India Ink) Teflon | Parallel | C-FEP (P) | 5 | | |
| M9W-T35 | Aluminized-Teflon (Al space facing)* | Parallel | Al/FEP (P) | 2 | | |
| M9W-T36 | Aluminized-Teflon (Al space facing)* | Parallel | Al/FEP (P) | 2 | 4 | 5 |
| M9W-T37 | Aluminized-Teflon (Al space facing)* | Parallel | Al/FEP (P) | 2 | | |
| M9W-T38 | Aluminized-Teflon (Al space facing)* | Parallel | Al/FEP (P) | 2 | | |

*FEP layer is space facing for all samples except Al/FEP (T35-T38)
^Silver-Teflon (FEP/Ag/Inconel)

Table 3. MISSE-9 PCE-1 Zenith Tensile Samples.

| MISSE-9 ID | Material | Parallel or Normal to Roll Lines | Abbreviation | Nominal Thickness (mils) | # Flight (F) Samples | # Control (C) Samples |
|---|---|---|---|---|---|---|
| M9Z-T1 | Aluminized-Teflon | Parallel | Al-FEP (P) | 2 | 4 | 3 |
| M9Z-T2 | Aluminized-Teflon | Parallel | Al-FEP (P) | 2 | | |
| M9Z-T3 | Aluminized-Teflon | Parallel | Al-FEP (P) | 2 | | |
| M9Z-T4 | Aluminized-Teflon | Parallel | Al-FEP (P) | 2 | | |
| M9Z-T5 | Aluminized-Teflon | Normal | Al-FEP (N) | 2 | 4 | 3 |
| M9Z-T6 | Aluminized-Teflon | Normal | Al-FEP (N) | 2 | | |
| M9Z-T7 | Aluminized-Teflon | Normal | Al-FEP (N) | 2 | | |
| M9Z-T8 | Aluminized-Teflon | Normal | Al-FEP (N) | 2 | | |
| M9Z-T9 | Aluminized-Teflon | Parallel | Al-FEP (P) | 5 | 4 | 3 |
| M9Z-T10 | Aluminized-Teflon | Parallel | Al-FEP (P) | 5 | | |
| M9Z-T11 | Aluminized-Teflon | Parallel | Al-FEP (P) | 5 | | |
| M9Z-T12 | Aluminized-Teflon | Parallel | Al-FEP (P) | 5 | | |
| M9Z-T13 | Aluminized-Teflon | Normal | Al-FEP (N) | 5 | 4 | 4 |
| M9Z-T14 | Aluminized-Teflon | Normal | Al-FEP (N) | 5 | | |
| M9Z-T15 | Aluminized-Teflon | Normal | Al-FEP (N) | 5 | | |
| M9Z-T16 | Aluminized-Teflon | Normal | Al-FEP (N) | 5 | | |
| M9Z-T17 | Carbon painted (India Ink) Teflon | Parallel | C-FEP (P) | 2 | 4 | 2 |
| M9Z-T18 | Carbon painted (India Ink) Teflon | Parallel | C-FEP (P) | 2 | | |
| M9Z-T19 | Carbon painted (India Ink) Teflon | Parallel | C-FEP (P) | 2 | | |
| M9Z-T20 | Carbon painted (India Ink) Teflon | Parallel | C-FEP (P) | 2 | | |
| M9Z-T21 | Aluminized-Teflon (Al space facing)* | Parallel | Al/FEP (P) | 2 | 4 | 2 |
| M9Z-T22 | Aluminized-Teflon (Al space facing)* | Parallel | Al/FEP (P) | 2 | | |
| M9Z-T23 | Aluminized-Teflon (Al space facing)* | Parallel | Al/FEP (P) | 2 | | |
| M9Z-T24 | Aluminized-Teflon (Al space facing)* | Parallel | Al/FEP (P) | 2 | | |

*FEP layer is space facing for all samples except Al/FEP (T21-T24)

Prior tests conducted on pristine 2 mil thick (0.0051 cm) Al-FEP samples as part of the MISSE-7 experiments showed a clear difference in the stress-strain curves for the samples punched out parallel to the roll direction (P), as compared to samples punched out normal to the roll direction (N).[17] The roll direction is the direction of the sheet of film being extruded. It is thought that more of the polymer molecules are aligned parallel to the roll direction than perpendicular to it. These differences can be seen in the stress-strain curves shown in Figure 13. The average ultimate tensile strength (UTS) and percent elongation at failure (%E) for pristine (i.e. control) samples punched out parallel to the roll direction was 29.8 ± 2.1 MPa and 218.1 ± 15.6%, respectively.[17] The average UTS and %E for control samples punched out normal to the roll direction was 25.5 ± 2.1 MPa and 270.9 ± 25.0%, respectively.[17] To study the effect of the roll direction on space environment degradation, the MISSE-9 PCE-1 experiment included Teflon FEP tensile samples that were cut both parallel and normal to the roll direction.

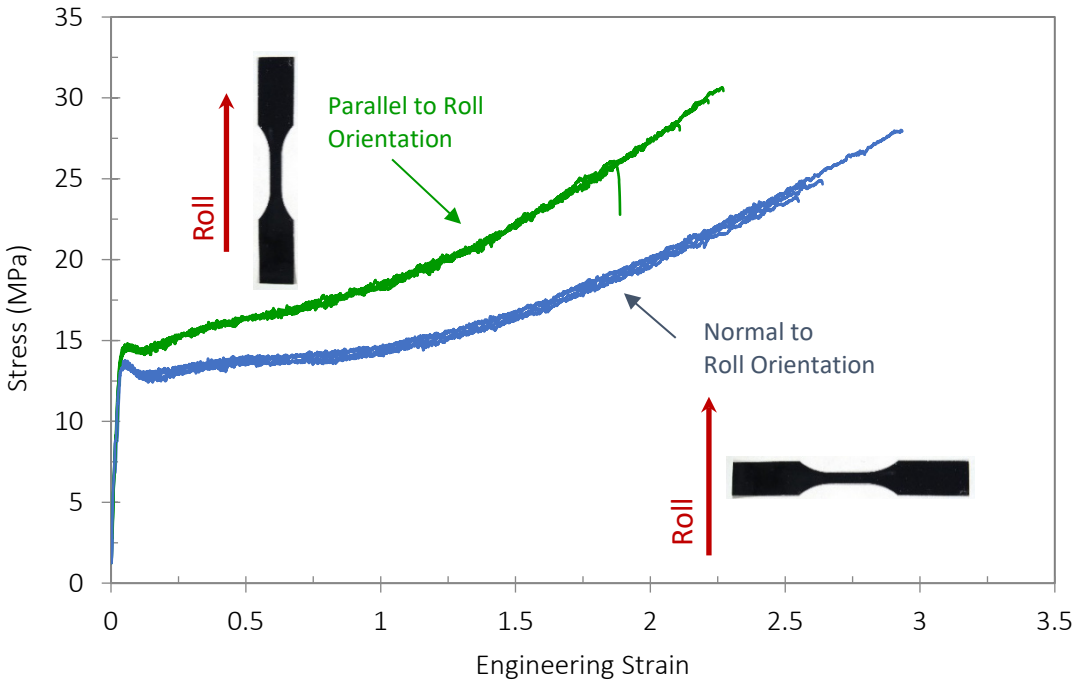


Figure 13. Stress-strain curves for 2-mil Al-FEP tensile samples punched out parallel to the roll direction (green) and samples punched out normal to the roll direction (blue).[17]

The MISSE-9 PCE-1 wake and zenith tensile samples included 2 and 5 mil thick Al-FEP cut both parallel and normal to the film roll direction to see the effect of the roll direction on space induced embrittlement. Four samples of Al-FEP were flown with the aluminized side facing the space direction (Al/FEP) to see if space radiation penetrates the Al film and embrittles the Teflon FEP. It included 5 mil silver-Teflon (FEP/Ag/Inconel (Ag-FEP)) samples cut parallel to the roll direction in the wake direction. And it included Teflon FEP (2 and 5 mil in wake, and 2 mil in zenith) that was carbon painted (India Ink) on the back surface (C-FEP) to see the effect of passive heating on the space radiation induced embrittlement.

### *MISSE-13 Polymers and Composites Experiment-4 (PCE-4)*

The MISSE-13 PCE-4 is a passive experiment with 98 samples that was flown in the wake (65 samples) and zenith (33 samples) directions. The primary objectives of the PCE-4 are to determine optical and mechanical property degradation of spacecraft materials and to assess the functionality of shape memory alloys, shape memory polymer composites, melanin-based composites and elastomer seal samples after radiation exposure in LEO. Like the PCEs 1-3, samples in the PCE-4 were included to determine the AO fluence in each mission orientation. Teflon FEP samples were used for contamination studies. A complete list of the PCE-4 samples is provided in Reference 18 along with additional experiment objectives and pre-flight photos of select PCE-4 experiment samples.

A pre-flight photograph of the PCE-4 samples loaded into the zenith (Z2 MSC 19 MS), wake mount side (W1 MSC 5 MS) and wake swing side (W1 MSC 5 SS) decks is shown in Figure 14. The PCE-4 samples in the wake MS deck are outlined in red. The larger white and

metallized square samples in MSC 5 MS are not part of the PCE-4. Figure 15 provides close-up photographs of the PCE-4 tensile samples flown on the W1 MSC 5 SS deck.

Figure 14. Pre-flight photograph of the MISSE-13 PCE-4 samples loaded into the MSC flight decks, from left to right: Z2 MSC 19 MS (zenith), W1 MSC 5 MS (wake) and W1 MSC 5 SS (wake). The PCE-4 samples in the wake MS deck are outlined in red.

A total of 24 wake tensile samples were flown as part of the PCE-4. Table 4 provides a list of the MISSE-13 PCE-4 wake tensile samples. The table provides the MISSE-13 sample identification (ID), material, material abbreviation and film thickness. The MISSE-13 PCE-14 wake tensile samples included 2 and 5 mil thick Teflon FEP to see the effect of space radiation on film thickness. Samples of both 2 mil and 5 mil thick Teflon FEP were AO treated on the back-surface to increase adhesion of a carbon coating. Thus, 2 and 5 mil thick Teflon FEP with an AO texture and carbon-coating (C-FEP, called FEP/C in reference 18) were included. And samples of 2 mil and 5 mil thick FEP that were AO treated on the back-surface were also flown without a carbon-coating to see if the AO treatment itself impacted the tensile properties of the FEP. Also flown were gossamer thin (0.2 mil thick) vapor deposited aluminum coated CP1 (VDA/CP1) solar sail material samples and 0.3 mil thick VDA/CP1-polytetrafluoroethylene (VDA/CP1-PTFE) composite solar sail material samples. The solar sail materials were flown with a Kapton support on either the front or back-surface in the grip area, one of which can be seen in Figure 15a. All the PCE-4 wake tensile samples were cut parallel to the roll direction. Like the MISSE-8 and MISSE-9 tensile samples, the flight and control tensile samples were punched from film sheets using a die fabricated to the specifications defined in the ASTM Standard D-638 for Type-V tensile specimens.[20] The manufacturer and material lot number for the flight sample material is provided in Table A-3 of the Appendix. Similar to the MISSE-9 samples, the MISSE-13 flight samples under-went pre-flight vacuum thermal testing at 60 °C for 24 hours at Aegis Aerospace. Similar

to the PCE-1 samples, the PCE-4 flight samples were also exempt from x-ray screening and the control samples were stored in ambient conditions at NASA Glenn during the flight mission.

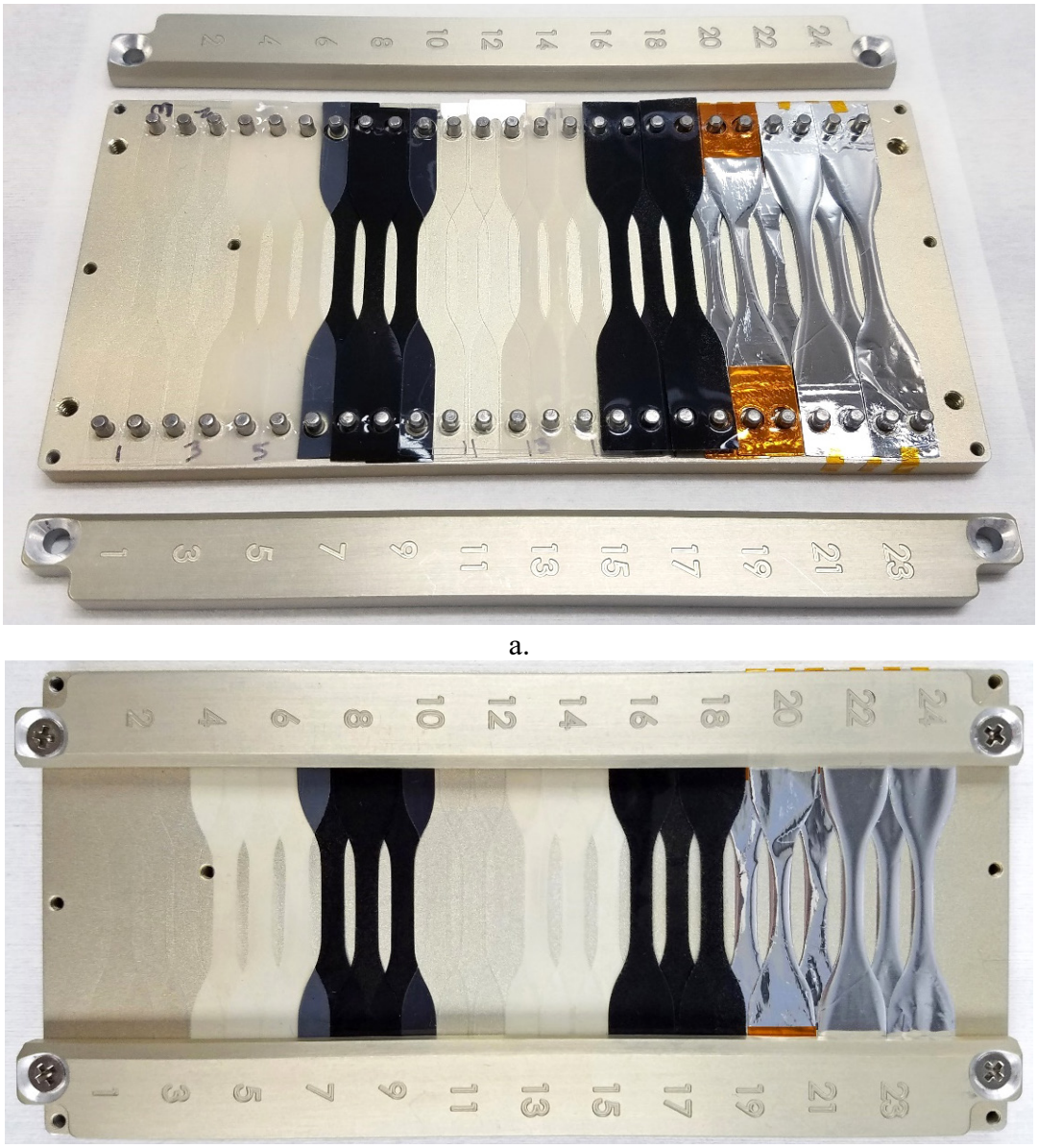


a.

b.

Figure 15. Pre-flight photographs of the MISSE-13 PCE-4 tensile samples loaded into the wake W1 MSC 5 SS flight deck: a). Image taken during sample loading showing holes and mounting pins in the grip area, and b). Final pre-flight assembly.

Table 4. MISSE-13 PCE-4 Wake Tensile Samples.

| MISSE-13 ID | Material | Abbreviation | Nominal Thickness (mils) | # Flight (F) Samples | # Control (C) Samples |
|---|---|---|---|---|---|
| M13W-T1 | Teflon (FEP) | FEP | 2 | | |
| M13W-T2 | Teflon (FEP) | FEP | 2 | 3 | 5 |
| M13W-T3 | Teflon (FEP) | FEP | 2 | | |
| M13W-T4 | Teflon (FEP) - AO textured on back surface | FEP-AO | 2 | | |
| M13W-T5 | Teflon (FEP) - AO textured on back surface | FEP-AO | 2 | 3 | 5 |
| M13W-T6 | Teflon (FEP) - AO textured on back surface | FEP-AO | 2 | | |
| M13W-T7 | Teflon (FEP) - AO textured and C coated on the back | C-FEP | 2 | | |
| M13W-T8 | Teflon (FEP) - AO textured and C coated on the back | C-FEP | 2 | 3 | 5 |
| M13W-T9 | Teflon (FEP) - AO textured and C coated on the back | C-FEP | 2 | | |
| M13W-T10 | Teflon (FEP) | FEP | 5 | | |
| M13W-T11 | Teflon (FEP) | FEP | 5 | 3 | 5 |
| M13W-T12 | Teflon (FEP) | FEP | 5 | | |
| M13W-T13 | Teflon (FEP) - AO textured on back surface | FEP-AO | 5 | | |
| M13W-T14 | Teflon (FEP) - AO textured on back surface | FEP-AO | 5 | 3 | 5 |
| M13W-T15 | Teflon (FEP) - AO textured on back surface | FEP-AO | 5 | | |
| M13W-T16 | Teflon (FEP) - AO textured and C coated on the back | C-FEP | 5 | | |
| M13W-T17 | Teflon (FEP) - AO textured and C coated on the back | C-FEP | 5 | 3 | 5 |
| M13W-T18 | Teflon (FEP) - AO textured and C coated on the back | C-FEP | 5 | | |
| M13W-T19 | VDA/CP1 solar sail material* | VDA/CP1 | 0.2 | | |
| M13W-T20 | VDA/CP1 solar sail material* | VDA/CP1 | 0.2 | 3 | 5 |
| M13W-T21 | VDA/CP1 solar sail material* | VDA/CP1 | 0.2 | | |
| M13W-T22 | VDA/CP1-PTFE composite solar sail material** | VDA/CP1-PTFE | 0. 3 | | |
| M13W-T23 | VDA/CP1-PTFE composite solar sail material** | VDA/CP1-PTFE | 0. 3 | 3 | 5 |
| M13W-T24 | VDA/CP1-PTFE composite solar sail material** | VDA/CP1-PTFE | 0. 3 | | |

*Kapton grip on front
**Kapton grip on back

# Experimental Procedures

### *Thickness Measurements*

A Heidenhain ND 280 digital thickness gauge (accuracy of ± 0.5 μm) was used to measure the thickness of control and tensile samples post-flight. The thickness was measured in five locations on each sample, and the average thickness was used to determine the cross-sectional area needed for calculating tensile stress. This is important as the samples can be eroded while in LEO. It should be noted that thickness measurements on some of the coated samples were difficult to obtain due to some of the coatings cracking, wrinkling, and flaking off (i.e. carbon coating). Thus, measurements were taken in areas where the coating was intact, and the sample would lay as flat as possible. This resulted in a larger scatter in the thickness measurements for these samples.

### *Tensile Properties*

An MTS Tytron 250 Electromechanical Test System (ETS) controlled by an MTS FlexTest SE controller was used for tensile testing. A 500N load cell was used when testing samples with a nominal thickness of 1 to 5 mil and a 50N load cell was used when testing samples with a nominal thickness of 0.2 or 0.3 mil. All samples were tested at room temperature with an elongation rate of 12.7 mm/min. The controller recorded load and displacement during each tension test.

From these data, the nominal strain at failure and ultimate tensile strength (UTS) were determined. The initial gauge length for the ASTM D638 Type V tensile samples (6.35 cm long) was 9.53 mm and the initial grip separation was 27 mm. The initial distance between shoulders of 25.4 mm was used to calculate nominal strain as the additional 2.5 mm of exposed material in the grip section has a larger cross section and does not contribute much to the nominal strain (≈0.2% strain) and 25.4 mm is best for comparing to previous MISSE and HST tensile data. Also, as mentioned previously, tensile stress was calculated based on the thickness of each sample measured using the Heidenhain ND 280 digital thickness gauge. The nominal strain to failure is referred to as the "percent elongation at failure (%E)" in this report even though it was not measured with an extensometer to be consistent with past MISSE tensile data. The %E values reported in this paper are calculated from the corrected zero-strain point after performing a toe compensation as described in ASTM standard D638.

## MISSE Mission Environmental Exposures

Table 5 provides the mission environmental exposure summary for the MISSE-8 Polymers Experiment, MISSE-9 PCE-1 and MISSE-13 PCE-4 tensile samples. The table provides the MISSE mission and flight experiment, location on ISS, flight direction (also referred to as flight orientation), MISSE carrier details, launch and return missions, and the dates of installation and retrieval. The table also provides for each carrier the direct space vacuum duration, direct space exposure duration (total time the carrier was open and exposed to the space environment), the computed AO fluence and solar exposure provided in total mission equivalent sun hours (ESH). Additional details on the mission exposures and AO fluence computations can be found in References 9 and 13.

Table 5. MISSE-8, MISSE-9 and MISSE-13 Tensile Sample Mission Exposure Summary.[9,13,21]

| MISSE Experiment | Location on ISS | Flight Direction | MISSE Carrier | Launch Mission | Installed on ELC-2 or MISSE-FF | Retrieved from ELC-2 or MISSE-FF | Return Mission | Space Vacuum Duration (Years) | Time on ELC-2 or MISSE-FF (Years) | Direct Space Exposure Duration (Years) | Atomic Oxygen Fluence (atoms/cm$^2$) | Mission Equivalent Sun Hours (ESH) |
|---|---|---|---|---|---|---|---|---|---|---|---|---|
| MISSE-8 Polymers Experiment | MISSE-8 ELC-2 Site 3 | Zenith | MISSE-8 PEC | STS-134 May 16, 2011 | May 20, 2011 | July 9, 2013 | SpaceX-3 May 18, 2014 | >2.14 | 2.14 | 2.14 | 1.96E+20 | 6100 |
| MISSE-9 PCE-1 | MISSE-FF | Wake | W3 (MSC 8) MS | SpaceX-14 April 2, 2018 | April 18, 2018 | April 26, 2019 | SpaceX-17 June 3, 2019 | 1.07 | 1.02 | 0.54 | 4.46E+16 | 634.6*-720# |
| | | Zenith | Z3 (MSC 5) MS | | April 19, 2018 | | | 1.07 | 1.02 | 0.54 | 3.19E+18 | 555.78*-1539# |
| MISSE-13 PCE-4 | MISSE-FF | Wake | W1 (MSC 5) SS | SpaceX-20 March 6, 2020 | March 18, 2020 | Nov. 27, 2020 | SpaceX-21 Jan. 13, 2021^ | 0.72 | 0.70 | 0.44 | 2.65E+18 | 515.6*-587# |

*Aegis Aerospace provided full mission ESH
#MISSE-8 ESH/year-based mission ESH
^January 13, 2021 EST (January 14, 2021 UTC)

The ESH estimates listed in Table 5 provided by Aegis Aerospace indicate that the wake samples received more solar exposure (MISSE-9 wake = 634.6 ESH) than the zenith samples (MISSE-9 zenith = 555.7 ESH). This is not consistent with expected zenith and wake exposures in LEO or with past MISSE environment exposure data such as the MISSE 7 wake and zenith solar estimates.[23] For the MISSE-7 mission, which was also located at ELC-2 Site 3, the estimated solar exposures were 2,000 ESH for the wake direction and 4,300 ESH for the zenith direction for a 1.5-year direct space exposure mission.[23] Tensile testing of Al-FEP samples from the MISSE-7 mission showed that samples flown in the zenith direction became more embrittled as a result of the increased solar exposure compared to wake samples.[17] The embrittlement trends observed in this study indicate that the MISSE-9 zenith samples received a significantly higher solar exposure than the wake samples. Thus, the Aegis ESH values are most likely not accurate, and ESH estimates were made for the MISSE-9 and MISSE-13 missions based on ESH values computed for the MISSE-8 (and MISSE-7) missions as discussed in reference 9. These MISSE-8 based ESH values, also provided in Table 5, are more consistent with expected flight orientation based solar exposures and with the PCE-1 and PCE-4 tensile trends reported here. The MISSE-8 ESH based MISSE-9 zenith ESH is significantly higher than the Aegis Aerospace provided MISSE-9 zenith ESH. The actual MISSE-9 zenith ESH is likely between these values. As stated in reference 9, the MISSE-8-based ESH values provided in Table 5 are the best ESH estimates available for the PCE 1-4. But it should be kept in mind that these values are lower than rough theoretical values for the wake orientations (≈18% lower) and higher than rough theoretical values for the zenith (≈21% higher) and nadir orientations.[9]

Contamination analyses for the PCE-1 and PCE-4 experiments are reported by de Groh in Reference 22. A summary of the Si atomic concentrations for samples flown along with the PCE-1 and PCE-4 tensile samples is provided in Table 6. As can be seen, the Si concentrations are relatively low indicating low level of molecular contamination.

Table 6. Silicon Atomic Concentrations for PCE-1 and PCE-4 Contamination Witness Samples.[22]

| MISSE Mission | Flight Orientation | Contamination Sample | Material | Time on MISSE-FF (Years) | Direct Space Exposure Duration (Years) | Si Atomic Concentration (at.%) |
|---|---|---|---|---|---|---|
| MISSE-9 | Wake | M9W-C3 F | $Al_2O_3$ | 1.02 | 0.54 | 1.7 |
| MISSE-9 | Zenith | M9Z-C3 F | $Al_2O_3$ | 1.02 | 0.54 | 1.5 |
| MISSE-13 | Wake | M13W-C4 F | Al-FEP | 0.70 | 0.44 | 1.6 |

# Results & Discussion

## *MISSE-8 Polymers Experiment*

### *Pre-flight and Post-Flight Photographs*

Figure 16 provides pre-flight (left) and post-flight (right) photographs of the MISSE-8 Polymers Experiment tensile samples. The Al-FEP samples warped (M8-7) as shown in Figure 16b. The carbon coating on the back surface of the C-FEP samples (M8-8) cracked and the samples are warped, as can be seen in Figure 16c. The CP1 samples discolored, as shown in Figure 16d. The clear FEP samples (M8-6 and M8-11) became slightly hazy.

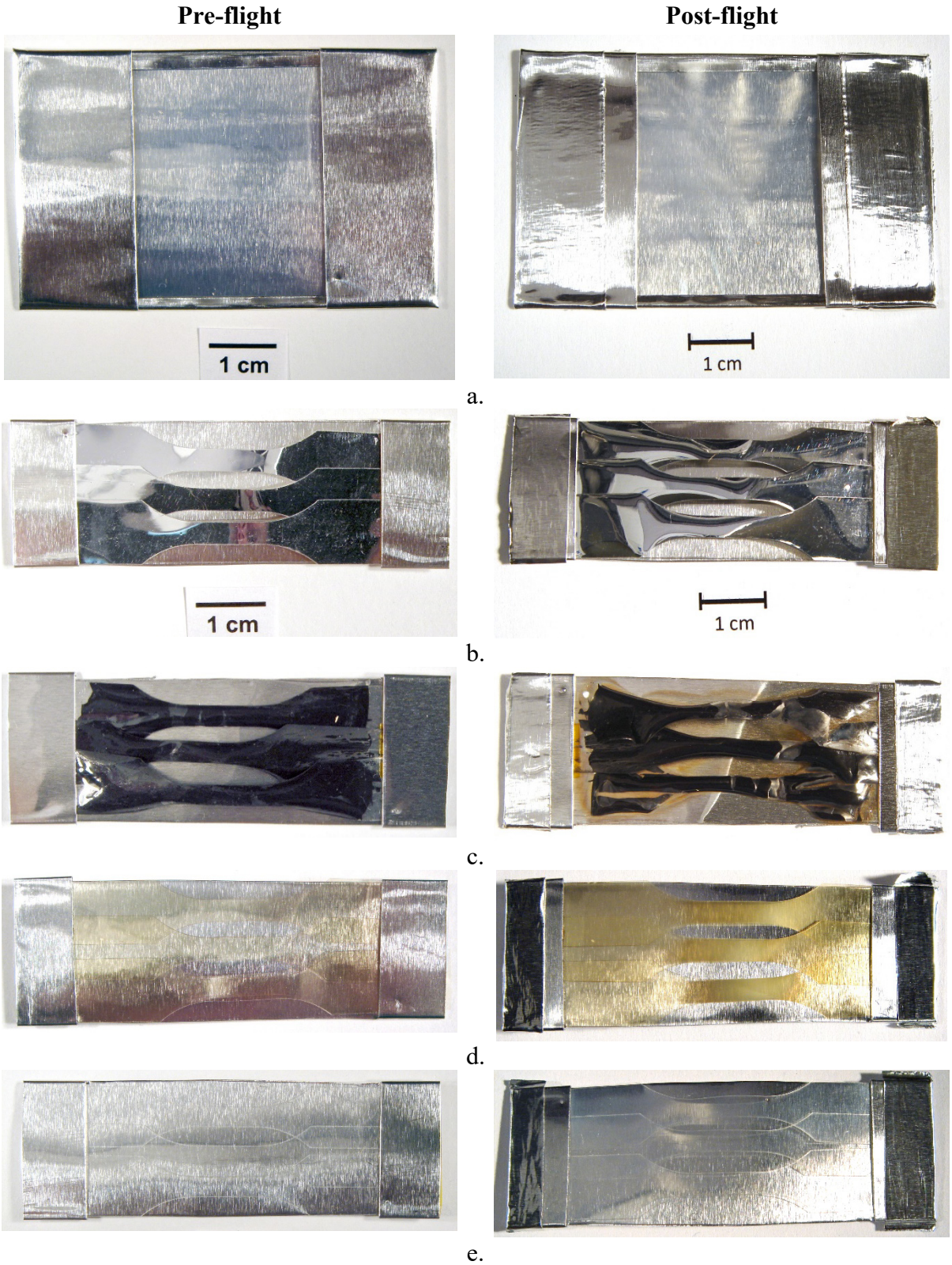


Figure 16. Pre-flight (left) and post-flight (right) photographs of the MISSE-8 Polymers Experiment tensile samples in their Al flight holders: a). Stacked Teflon FEP (M8-6), b). Al-FEP (M8-7), c). C-FEP (M8-8), d). CP1 (M8-9), and e). FEP (M8-11).

*Thickness Measurements*

Table 7 provides the average thickness measurements for the MISSE-8 Polymers Experiment zenith tensile flight and control samples. Table 7 provides MISSE ID, number of samples, material, flight or control sample, average thicknesses, standard deviation of thicknesses, and percent change in thickness of the flight samples as compared to the control samples.

Table 7. Thickness Data for the MISSE-8 Polymers Experiment Zenith Tensile Samples.

| MISSE Sample ID (#) | # of Samples | Material | Flight or Control | AVG Thickness (mils) | Std. Dev. (mils) | Flight vs. Control Thickness (% Change) |
|---|---|---|---|---|---|---|
| M8-6 Layer 1-1 to 1-3 F | 3 | 2 mil FEP | Flight Top Layer | 1.84 | 0.02 | -4.1 |
| M8-6 Layer 2-1 to 2-3 F | 3 | | Flight 2nd Layer | 1.97 | 0.04 | 2.9 |
| M8-6 Layer 3-1 to 3-3 F | 3 | | Flight 3rd Layer | 1.98 | 0.04 | 3.4 |
| M8-6 Layer 4-1 to 4-3 F | 3 | | Flight 4th Layer | 1.91 | 0.01 | -0.2 |
| M8-6 Layer 5-1 to 5-3 F | 3 | | Flight 5th Layer | 1.94 | 0.01 | 1.4 |
| M8-6 Layer 6-1 to 6-3 F | 3 | | Flight 6th Layer | 2.04 | 0.02 | 6.5 |
| M8-6-1 to M8-6-4 (N) C | 4 | | Control | 1.91 | 0.02 | N/A |
| M8-7-1 to M8-7-3 F | 3 | 2 mil Al-FEP | Flight | 1.79 | 0.03 | -9.2 |
| M8-7-1 to M8-7-6 C | 6 | | Control | 1.97 | 0.06 | |
| M8-8-1 to M8-8-3 F | 3 | 2 mil C-FEP | Flight | 3.52 | 0.51 | N/A (no coated control) |
| M8-8-1 to M8-8-3 C | 3 | | Control | 1.92 | 0.01 | |
| M8-9-1 to M8-9-3 F | 3 | 1 mil CP1 | Flight | 0.81 | 0.03 | -11.4 |
| M8-9-1 to M8-9-6 C | 6 | | Control | 0.91 | 0.01 | |
| M8-11-1 to M8-11-3 F | 3 | 2 mil FEP | Flight | 1.92 | 0.01 | 0.2 |

* M8-6 (M8-6-1 to M8-6-4 (N) C) was used as the control samples for M8-11

The majority of the zenith flight samples had measurable thickness loss after space exposure. The fairly high MISSE-8 zenith AO fluence of 1.96 x $10^{20}$ atom/cm$^2$ likely contributed to the thickness loss.[13] The space-exposed top layer of the stacked Teflon FEP samples (M8-6 L1 F) was 4.1% thinner than the average thickness of the control. The average thickness for the underlying layers (Layer 2 - 6) ranged from -0.2% to 6.5% as compared to control samples, indicating no erosion of the underlying layers. The average Al-FEP flight sample (M8-7 F) thickness was 9.2% thinner than the average thickness of the control samples. There was no carbon coating on the control samples for the C-FEP flight samples, so thickness comparisons were not made. The average CP1 flight sample (M8-9 F) thickness was 11.4% thinner than the average thickness of the control samples. The average FEP flight sample (M8-11 F) thickness was 0.2% thicker than the average thickness of the M8-6 control samples. It should be noted that the M8-9 F CP1 flight samples felt sticky post-flight.

*Tensile Results*

The roll direction of the MISSE-8 flight FEP samples (M8-6 and M8-11) was not noted when the samples were die-cut from film sheets. Therefore, control samples were cut from the stacked FEP control film materials in both the parallel (M8-6-1 to M8-6-3 (P) C) and normal (M8-6-1 to M8-6-4 (N) C) directions, so both sets of data would be available. It should be noted that tensile data for M8-6-3 (N) C was not included due to a software crash during the test. Table 8 provides the tensile data for the 2 mil FEP normal and parallel samples. As can be seen in Figure 17, and as listed in Table 8, the MISSE-8 control FEP samples show the same trends shown in Figure 13 for the MISSE-7 pristine (control) 2 mil FEP samples, with the Parallel (P) samples (light and dark green) having a higher UTS and a lower %E than the Normal (N) samples (blues and purple).

Table 8. Tensile Data for 2 mil FEP Parallel and Normal Control Samples.

| MISSE-8 ID | Material | Parallel or Normal to Roll Lines | Elastic Modulus (MPa) | Yield Strength (MPa) | UTS (MPa) | Ave. UTS (MPa) | %E | Ave. %E |
|---|---|---|---|---|---|---|---|---|
| M8-6-1 (N) C | FEP | Normal | 639.71 | 12.05 | 25.98 | 27.40 ± 1.77 | 244.08 | 258.19 ± 14.20 |
| M8-6-2 (N) C | | | 659.26 | 12.35 | 29.39 | | 272.48 | |
| M8-6-4 (N) C | | | 611.86 | 11.70 | 26.84 | | 258.00 | |
| M8-6-1 (P) C | FEP | Parallel | 632.38 | 12.17 | 30.64 | 31.22 ± 2.20 | 207.74 | 210.94 ± 15.10 |
| M8-6-2 (P) C | | | 625.04 | 11.95 | 29.36 | | 197.70 | |
| M8-6-3 (P) C | | | 616.44 | 12.05 | 33.65 | | 227.39 | |

The MISSE-8 tensile data is provided in Table 9. The table includes the MISSE-8 tensile sample ID, whether it is a flight (F) or control (C) sample, material, nominal film thickness, elastic modulus, yield strength, ultimate tensile strength (UTS), average UTS with standard deviation, percent change in average flight UTS as compared to the control, percent elongation to failure (%E), average %E with standard deviation, and the percent change in average flight %E as compared to the control. As can be seen in Figure 17, a flight sample from each of the top three layers (red, orange, and yellow) of the multilayered M8-6 sample follow the stress-strain curves of the control samples sectioned normal to the roll direction (N). Therefore, the M8-6 flight samples were most likely cut normal to the roll direction and their tensile properties are compared to the control samples cut normal to the roll direction in Table 9.

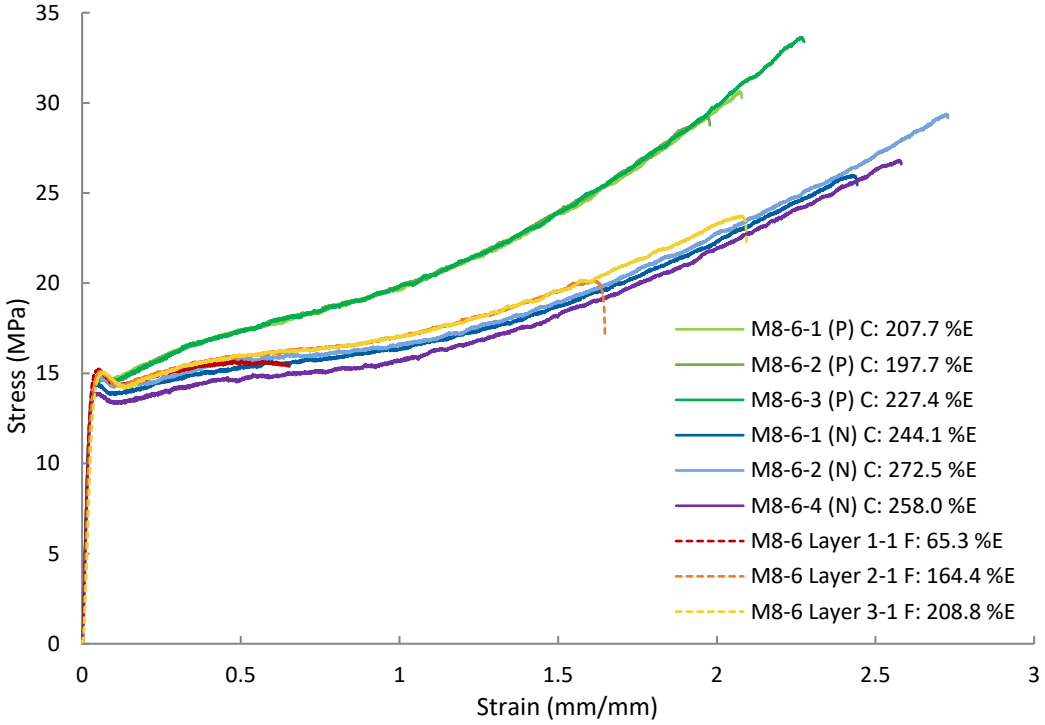


Figure 17. Stress-strain curves for numerous M8-6 (2 mil FEP) flight and control samples.

Figure 18 provides stress-strain curve for the three M8-7 (2 mil Al-FEP) flight samples (M8-7-1 F to M8-7-3 F) along with four of the six M8-7 control samples (M8-7-1 C to M8-7-4 C). As can be seen (and as listed in Table 9), the 2 mil thick Al-FEP flight samples are very embrittled after 2.14 years of zenith space exposure with an average %E of 34.86 ± 5.04, which is an 86.1% decrease in the %E as compared to the control samples (251.35 ± 16.07 %E).

Table 9. Tensile Data for the MISSE-8 Tensile Samples.

| MISSE-8 ID | Flight or Control | Material | Thickness (mils) | Elastic Modulus (MPa) | Yield Strength (MPa) | UTS (MPa) | Ave. UTS (MPa) | Percent Change in UTS | % Elong. (%E) | Ave. %E | Percent Change in %E |
|---|---|---|---|---|---|---|---|---|---|---|---|
| M8-6 Layer 1-1 | F | FEP | 2 | 663.80 | 12.43 | 15.70 | 15.69 ± 0.01 | -42.7 | **65.32** | 67.81 ± 3.66 | -73.7 |
| M8-6 Layer 1-2 | F | | | 683.05 | 12.56 | 15.69 | | | **66.09** | | |
| M8-6 Layer 1-3 | F | | | 654.39 | 12.25 | 15.69 | | | **72.01** | | |
| M8-6 Layer 2-1 | F | FEP | 2 | 622.84 | 11.83 | 20.15 | 24.31 ± 3.62 | -11.3 | **164.38** | 213.57 ± 42.69 | -17.3 |
| M8-6 Layer 2-2 | F | | | 627.00 | 11.86 | 26.73 | | | **241.02** | | |
| M8-6 Layer 2-3 | F | | | 622.81 | 12.01 | 26.06 | | | **235.30** | | |
| M8-6 Layer 3-1 | F | FEP | 2 | 504.04 | 12.21 | 23.76 | 23.99 ± 1.08 | -12.5 | **208.78** | 210.50 ± 11.53 | -18.5 |
| M8-6 Layer 3-2 | F | | | 615.01 | 11.93 | 25.17 | | | **222.79** | | |
| M8-6 Layer 3-3 | F | | | 619.42 | 11.88 | 23.04 | | | **199.93** | | |
| M8-6 Layer 4-1 | F | FEP | 2 | 636.38 | 11.38 | 23.59 | 23.75 ± 0.49 | -13.3 | **215.98** | 218.03 ± 6.29 | -15.6 |
| M8-6 Layer 4-2 | F | | | 639.98 | 11.47 | 23.36 | | | **213.01** | | |
| M8-6 Layer 4-3 | F | | | 636.74 | 11.27 | 24.30 | | | **225.09** | | |
| M8-6 Layer 5-1 | F | FEP | 2 | 635.95 | 11.41 | 24.84 | 24.36 ± 0.77 | -11.1 | **229.40** | 224.80 ± 7.36 | -12.9 |
| M8-6 Layer 5-2 | F | | | 632.48 | 11.48 | 24.76 | | | **228.70** | | |
| M8-6 Layer 5-3 | F | | | 624.24 | 11.20 | 23.47 | | | **216.31** | | |
| M8-6 Layer 6-1 | F | FEP | 2 | 636.95 | 11.05 | 22.78 | 22.96 ± 0.58 | -16.2 | **211.72** | 213.03 ± 6.89 | -17.5 |
| M8-6 Layer 6-2 | F | | | 629.18 | 11.30 | 23.60 | | | **220.49** | | |
| M8-6 Layer 6-3 | F | | | 627.84 | 11.18 | 22.49 | | | **206.89** | | |
| M8-6-1 (N) | C | FEP (N) | 2 | 639.71 | 12.05 | 25.98 | 27.40 ± 1.77 | N/A | **244.08** | 258.19 ± 14.20 | N/A |
| M8-6-2 (N) | C | | | 659.26 | 12.35 | 29.39 | | | **272.48** | | |
| M8-6-4 (N) | C | | | 611.86 | 11.70 | 26.84 | | | **258.00** | | |
| M8-7-1 | F | Al-FEP* | 2 | 769.09 | 13.62 | 16.36 | 16.63 ± 0.23 | -55.1 | **34.86** | 34.86 ± 5.04 | -86.1 |
| M8-7-2 | F | | | 776.85 | 13.44 | 16.74 | | | **39.90** | | |
| M8-7-3 | F | | | 785.41 | 13.86 | 16.78 | | | **29.83** | | |
| M8-7-1 | C | Al-FEP* | 2 | 700.11 | 12.87 | 34.52 | 37.05 ± 2.19 | | **232.19** | 251.35 ± 16.07 | |
| M8-7-2 | C | | | 701.56 | 12.89 | 35.04 | | | **238.17** | | |
| M8-7-3 | C | | | 701.63 | 12.68 | 38.99 | | | **266.53** | | |
| M8-7-4 | C | | | 690.56 | 12.81 | 38.92 | | | **266.67** | | |
| M8-7-5 | C | | | 703.78 | 12.91 | 39.17 | | | **264.18** | | |
| M8-7-6 | C | | | 702.30 | 12.94 | 35.68 | | | **240.34** | | |
| M8-8-1 | F | C-FEP* | 2 | 992.87 | 8.56 | 8.82 | 7.49 ± 1.20 | -66.5 | **2.04** | 1.98 ± 0.10 | -99.1 |
| M8-8-2 | F | | | 558.59 | 6.22 | 6.49 | | | **1.86** | | |
| M8-8-3 | F | | | 437.88 | 6.58 | 7.15 | | | **2.04** | | |
| M8-8-1 | C | C-FEP* | 2 | 600.37 | 11.41 | 25.06 | 22.34±2.62 | | **247.64** | 213.57 ± 31.97 | |
| M8-8-2 | C | | | 597.44 | 11.40 | 19.83 | | | **184.23** | | |
| M8-8-3 | C | | | 602.42 | 11.48 | 22.12 | | | **208.85** | | |

Table 9. Tensile Data for the MISSE-8 Tensile Samples.

| MISSE-8 ID | Flight or Control | Material | Thickness (mils) | Elastic Modulus (MPa) | Yield Strength (MPa) | UTS (MPa) | Ave. UTS (MPa) | Percent Change in UTS | % Elong. (%E) | Ave. %E | Percent Change in %E |
|---|---|---|---|---|---|---|---|---|---|---|---|
| M8-9-1 | F | CP1 | 1 | 2965.79 | 72.37 | 92.14 | 92.20 ± 2.66 | -17.8 | **4.91** | 4.58 ± 0.30 | -33.3 |
| M8-9-2 | F | | | 2995.95 | 71.45 | 89.58 | | | **4.32** | | |
| M8-9-3 | F | | | 3217.95 | 75.43 | 94.89 | | | **4.50** | | |
| M8-9-1 | C | CP1 | 1 | 3356.20 | 79.62 | 112.22 | 112.17 ± 0.26 | | **7.01** | 6.86 ± 0.16 | |
| M8-9-3 | C | | | 3365.92 | 79.44 | 112.25 | | | **6.89** | | |
| M8-9-4 | C | | | 3374.51 | 78.20 | 111.79 | | | **6.64** | | |
| M8-9-5 | C | | | 3369.12 | 78.89 | 112.40 | | | **6.89** | | |
| M8-11-1 | F | FEP | 2 | 653.74 | 12.10 | 14.53 | 14.53 ± 0.01 | -47.0^ | **43.74** | 40.89 ± 2.91 | -84.2^ |
| M8-11-2 | F | | | 662.77 | 12.17 | 14.53 | | | **37.93** | | |
| M8-11-3 | F | | | 654.37 | 12.20 | 14.52 | | | **41.00** | | |

* FEP layer is space facing

^ Compared with M8-6 (N) control average

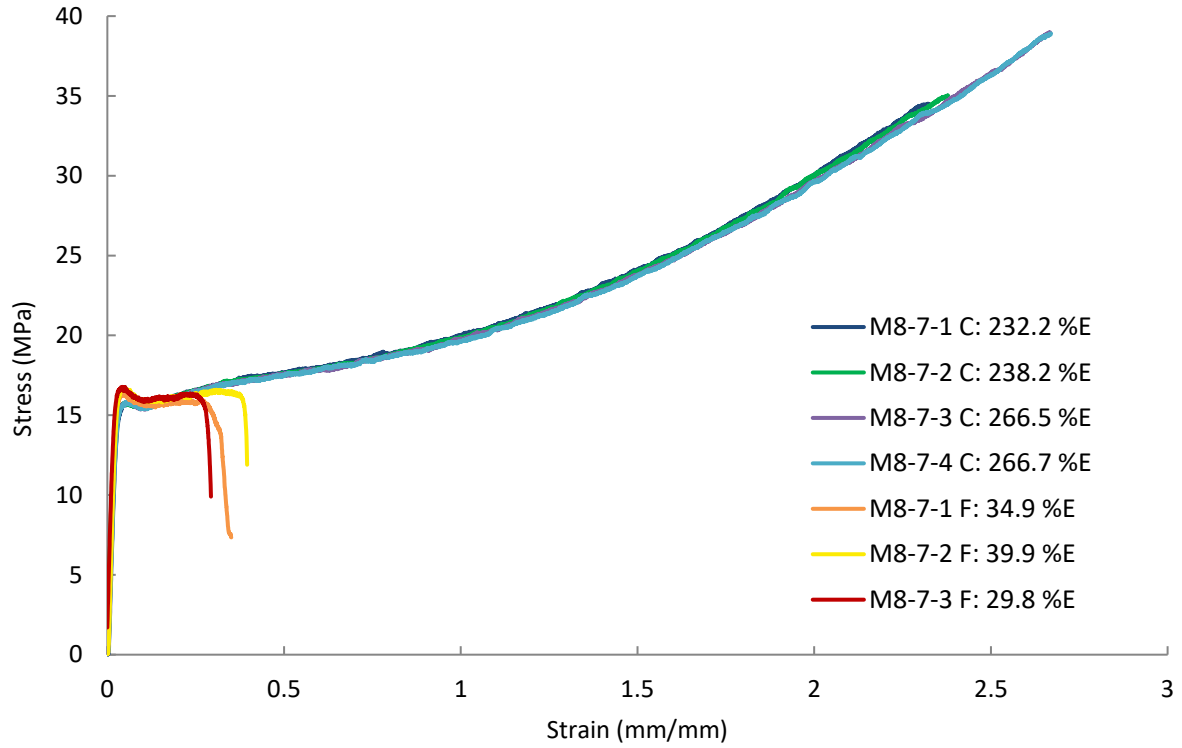


Figure 18. Stress-strain curves for M8-7 (2 mil Al-FEP) flight and control samples.

The die-cut direction of the M8-11 (2 mil FEP) flight tensile samples was not indicated pre-flight. As shown in Figure 19, the flight samples' stress-strain curves follow the M8-6 2 mil FEP normal control samples' stress-strain curves. Thus, the flight samples' average UTS and %E is compared to the M8-6 normal control samples in Table 9. Like the other MISSE-8 zenith Teflon FEP samples, the 2 mil FEP flight samples are very embrittled after 2.14 years of zenith space exposure with an average %E of 40.89 ± 2.91, which is an 84.2% decrease in the %E as compared to the control samples (258.19 ± 14.20 %E).

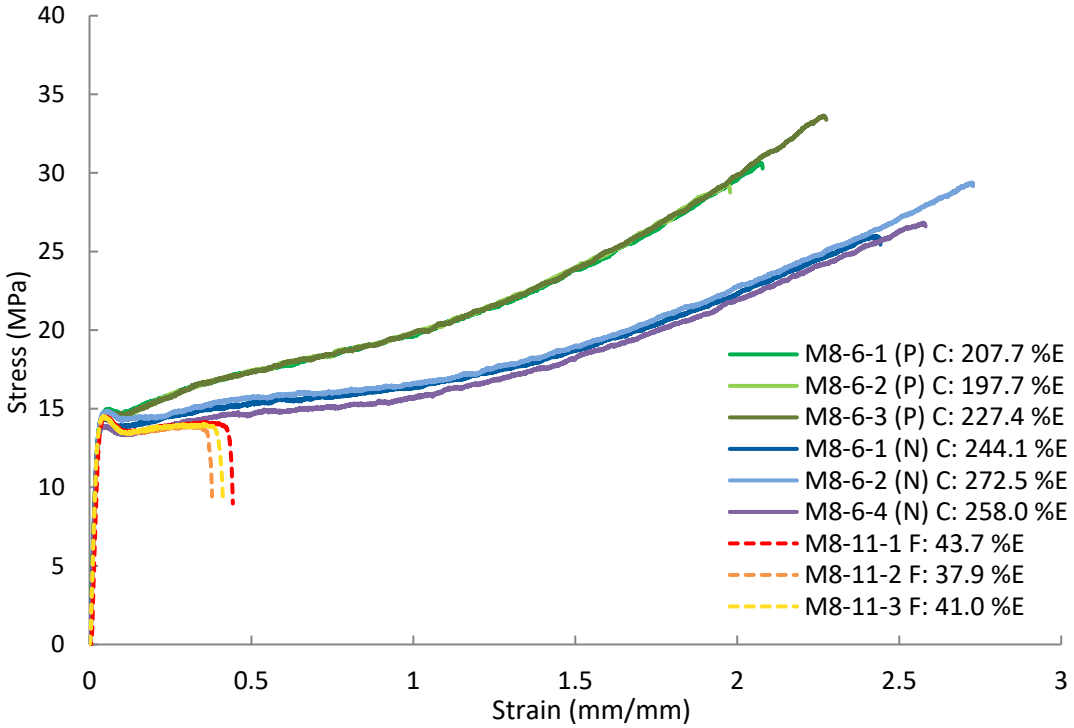


Figure 19. Stress-strain curves for M8-11 (2 mil FEP) flight and M8-6 control samples.

Figure 20 provides stress-strain curve for the three M8-8 (2 mil C-FEP) flight samples (M8-8-1 F to M8-8-3 F) along with the three M8-8 control samples (M8-8-1 C to M8-8-3 C). The C-FEP samples are extremely embrittled, with almost no remaining ductility and a large decrease in strength. The average %E for these flight samples was only 1.98 ± 0.10 %E, which is an 99.1% decrease in the %E as compared to the control samples (213.57 ± 31.07 %E). It should be noted that the control C-FEP samples had a wider spread in the elongation data (184.23 to 247.64 %E), and thus a greater standard deviation (31.97 %E) than the Al-FEP samples, which had a standard deviation of 16.07 %E.

The MISSE-8 C-FEP flight data, is consistent with prior flight and ground-test data and indicates that the increased on-orbit passive heating of the black C-FEP caused significantly increased embrittlement of FEP in LEO.[17] A study conducted by de Groh et al. showed that vacuum thermal exposure alone did not cause embrittlement of Teflon FEP, while radiation exposure with resulting scission damage causes FEP embrittlement, and that there is a synergistic effect of greater radiation induced embrittlement with higher corresponding thermal exposures.[24] The importance of the thermal exposure on the increased embrittlement of irradiated Teflon FEP was also reported by a HST MLI Failure Review Board (FRB) that conducted analyses of retrieved HST MLI and ground-tests after Servicing Mission 2 (SM2) astronauts found severely degraded MLI. The FRB concluded that *"the observations of HST MLI and ground testing of pristine samples indicate that thermal cycling with deep-layer damage from electron and proton radiation are necessary to cause the observed Teflon® FEP embrittlement and the propagation of cracks along stress concentrations. Ground testing and analysis of retrieved MLI indicate that damage increases with the combined total dose of electrons, protons, ultraviolet and x-ray radiation along with thermal cycling.*[6]"

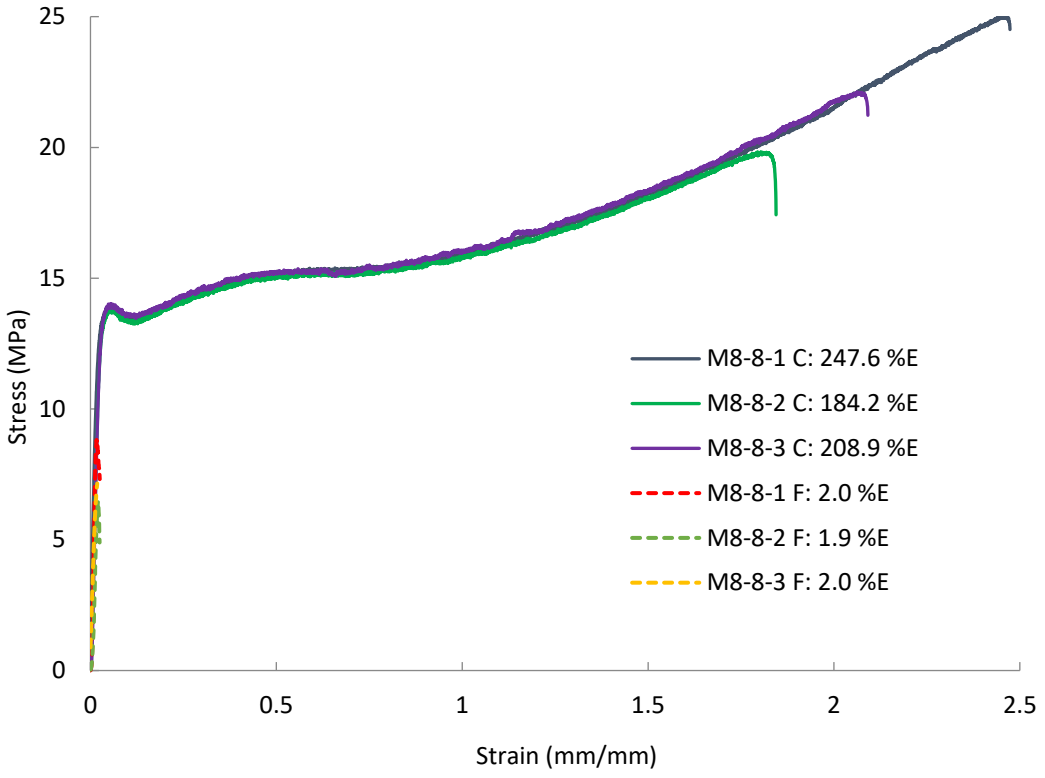


a.

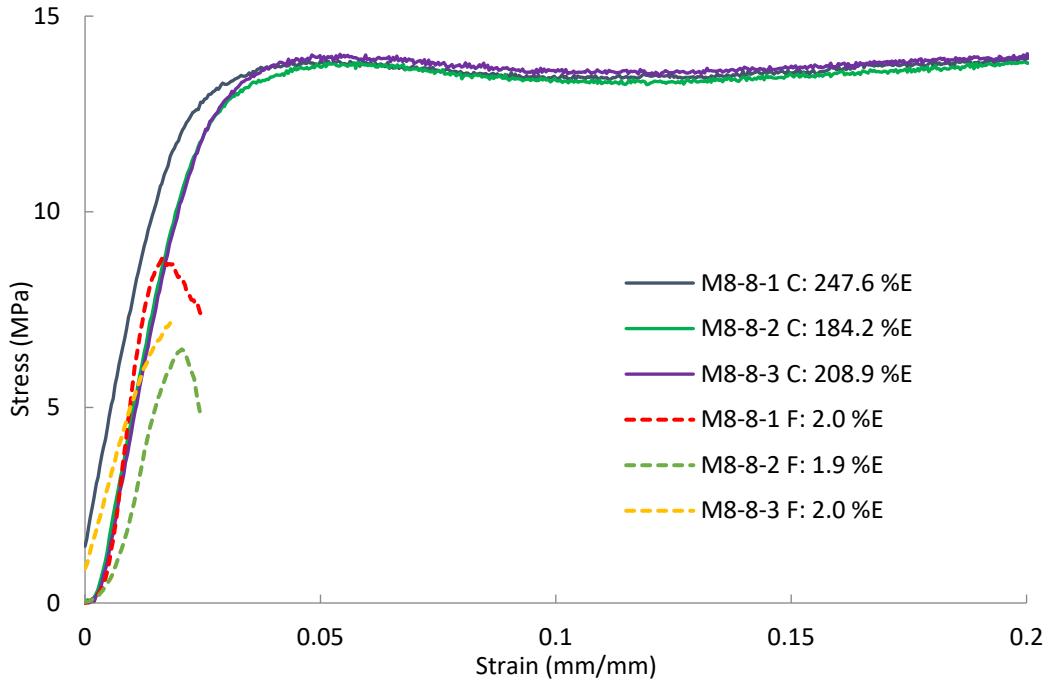


b.

Figure 20. Stress-strain curves for M8-8 (2 mil C-FEP) flight and control samples: a). Full strain scale (0.0-2.5 mm/mm) showing control sample curves, and b). Close-up (0.0-0.2 mm/mm) strain showing severely embrittled flight sample curves.

Figure 21 is a bar chart showing the average %E values, with standard deviation error bars, for the MISSE-8 2 mil Teflon FEP flight and control samples. As can be seen, the control averages for the clear FEP (258.2 %E) and Al-FEP (251.2 %E) are very similar, and the C-FEP is somewhat lower (213.6 %E) but has twice the standard deviation (32%) of the clear FEP (14.2 %E) or Al-FEP (16.1%). Zenith space exposure over 2.14 years significantly embrittled the FEP and Al-FEP samples (34.9-67.8 %E) and greatly embrittled (1.98 %E) black C-FEP samples.

The results from the M8-6 multilayered 2 mil thick Teflon FEP sample were interesting. The average %E of the Layer 1 (space-exposed) samples was 67.81 ± 3.66, which was a 73.7% decrease as compared to the control samples (258.19 ± 14.20 %E). Notably, all five of the underlying layers were embrittled to a lesser extent, and to a somewhat similar level. Layers 2-6 showed 210.50 - 224.80 %E, a decrease of 12.9-18.5 % as compared to the control samples. A similar flight study with more tensile samples per layer could allow the determination of any significant trends in the embrittlement of these layers.

The M8-6 Layer 1 and M8-11 samples were fabricated from the same batch of FEP and directly exposed to space for the same duration, so it was expected that they would be embrittled to the same extent. However, the M8-6 Layer 1 samples were slightly less embrittled than the M8-11 samples. A factor that may have led to the difference in embrittlement is that the M8-6 layered tensile samples were die-cut into tensile samples post-flight, while the other samples were die-cut into tensile samples prior to flight. As such, a potential explanation for the greater embrittlement of the M8-7 and M8-11 samples is that exposing the tensile sample edges to space further embrittles the edges of the samples, leading to an early onset of failure during testing.

Past research conducted on Teflon FEP indicates that VUV radiation (>170 nm), soft x-rays in the energy range of solar flare x-rays (1500–3000 eV), and electron and proton radiation (i.e. LEO trapped particle radiation (> 40 keV)), can all cause deep layer damage in Teflon FEP with decreases in mechanical properties.[24-26] Dever, et al. found that the absorbed dose of electrons in Teflon FEP in LEO (which is significantly greater than the absorbed proton dose) is greatest near the surface, but a significant dose is deposited into the bulk of 5 mil (127 μm) thick FEP.[25] For example, Dever found the computed trapped electron dose in Hubble Space Telescope Teflon FEP from launch in April 1990 to 2010 was 2036.0 krad at a depth of 0.001 mm (0.04 mils) and 318.5 krad at a depth of 0.127 mm (5 mil), with the dose following an exponential decrease versus depth for 5 mil Teflon FEP.[25] Solar flare x-rays also have a higher absorption at the surface but penetrate deeper into FEP.[24,27] These findings are consistent with the M8-6 layered Teflon FEP results that show the most damage in the top 2 mil (50.8 μm) layer and a much lower level of embrittlement in the underlying layers.

Past research has also shown that vacuum irradiated Teflon FEP (Al-FEP) tensile samples experience further embrittlement when later exposed to air for long periods, as compared to samples similarly irradiated and stored under vacuum.[28] As the samples in this study were stored in air post-flight, Teflon FEP that remains in LEO may be less embrittled than the samples in this study.

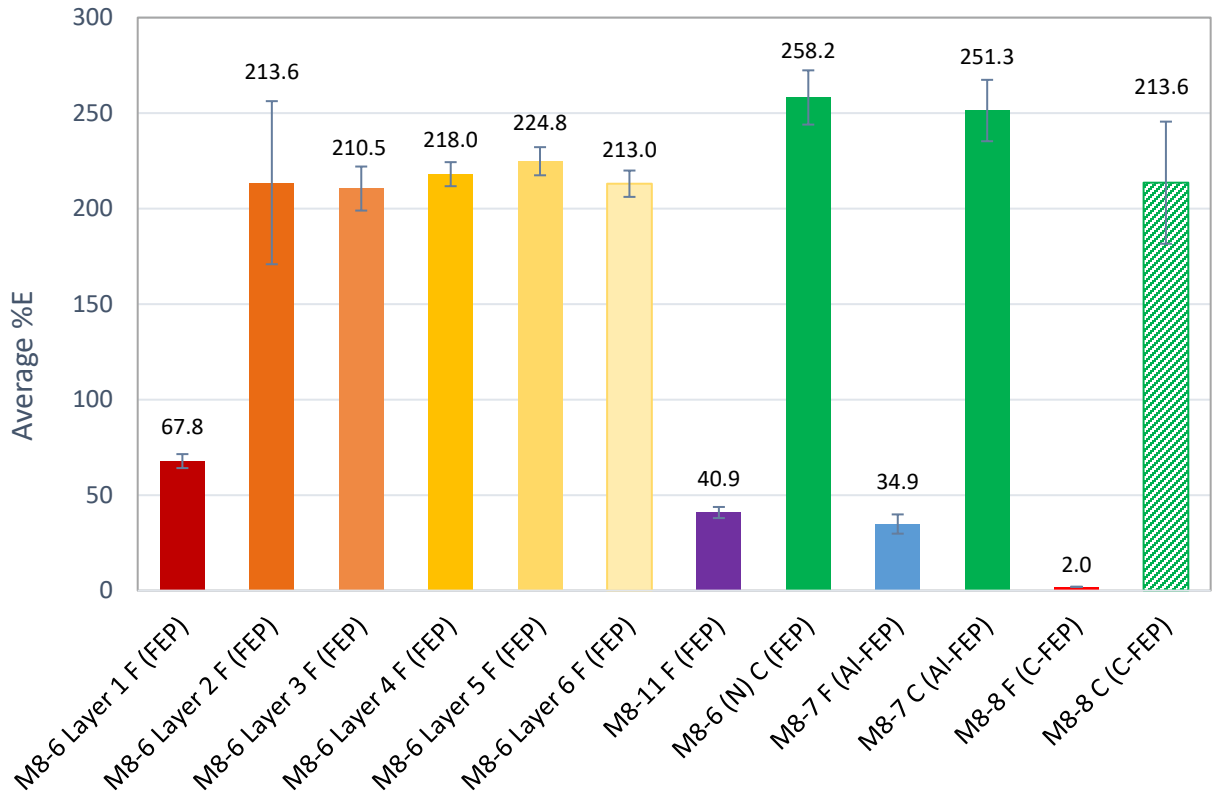


Figure 21. Bar chart showing the average %E for the MISSE-8 2 mil Teflon FEP flight (F) and control (C, green) samples.

Figure 22 provides stress-strain curves for the three M8-9 (1 mil CP1) flight samples (M8-9-1 F to M8-9-3 F) along with four of the six M8-9 control samples. The M8-9-2 C control failed at about the same point as the other control samples, as indicated by the drop in load, but held on by a thread for a while before failing completely. Also, the M8-9-6 C control sample's stress-strain curve was significantly different than the other control samples and was considered an outliner. Thus the %E for M8-9-2 C and M8-9-6 C were not included in the averages. As can be seen, and as listed in Table 9, the 1 mil CP1 flight samples were also embrittled with an average %E of 4.58 ± 0.30, which is an 33.3% decrease in the %E as compared to the control samples (6.86 ± 0.16 %E).

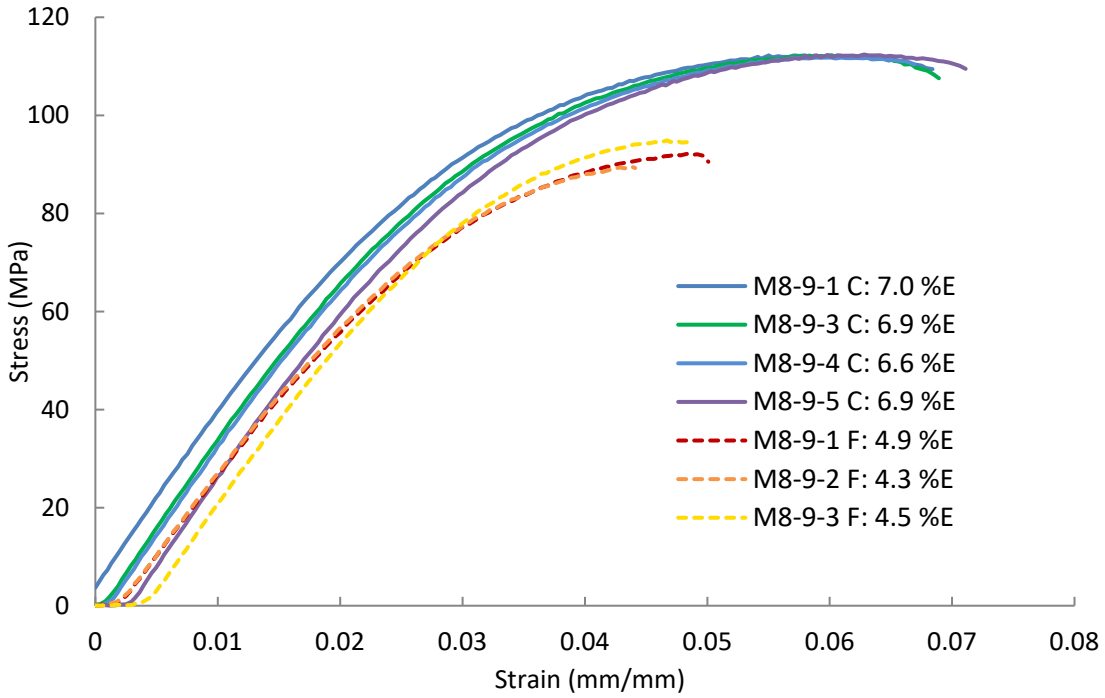


Figure 22. Stress-strain curves for M8-9 (1 mil CP1) flight and control samples.

### *MISSE-9 Polymers and Composites Experiment-1 (PCE-1)*

*On-Orbit Photos*

On-orbit photographs were taken once a month during the MISSE-9 mission. Example photographs of a section of the MISSE-9 wake tensile samples are provided in Figure 23. These images were taken on April 23, 2018 (Figure 23a) shortly after deployment on April 19, 2018, and on December 26, 2018 (Figure 23b) shortly after the final closure. The on-orbit photographs revealed that two of the MISSE-9 PCE-1 wake C-FEP samples broke while on-orbit, which indicates the samples were greatly embrittled. The MISSE-9 PCE-1 wake and zenith metallized Teflon tensile samples were shown to be intact.

a. b.

Figure 23. Examples of on-orbit photographs of a section of the MISSE-9 PCE-1 wake tensile samples: a). Image taken on April 24, 2018 shortly after deployment, and b). Image taken on December 26, 2018 shortly after the final closure of the MSC.

The series of on-orbit images was used to determine the amount of space exposure that the C-FEP samples experienced before failure. Figure 24 provides on-orbit images of the MISSE-9 PCE-1 wake C-FEP samples (M9W-T26 to M9W-T34) over time. The images were taken on July 25, 2018 (Figure 24a) showing no broken samples, August 27, 2018 (Figure 24b) showing M9W-T34 is broken, October 29, 2018 (Figure 24c) showing M9W-T31 is broken, and December 26, 2018 (Figure 24d) showing that M9W-T29 is cracked. Thus, the on-orbit images showed that one 5 mil thick C-FEP sample (M9W-T34) broke on-orbit after ≈97 days (0.27 years) of direct space exposure and another (M9W-T31) broke after ≈154 days (0.42 years) of direct space exposure. In addition, the 2 mil thick C-FEP sample (M9W-T29) appears to have cracked after 0.54 years of space exposure. It should be noted that the direct space exposure time does not directly correspond to the calendar dates because the MSCs are opened and closed throughout the mission. These on-orbit broken C-FEP samples indicate that the higher on-orbit temperature caused by the carbon coating results in a synergistic effect that increases the radiation-induced embrittlement of Teflon FEP in LEO. This result is consistent with prior MISSE tensile data (i.e. MISSE-7)[17] and the MISSE-8 results discussed in the previous section.

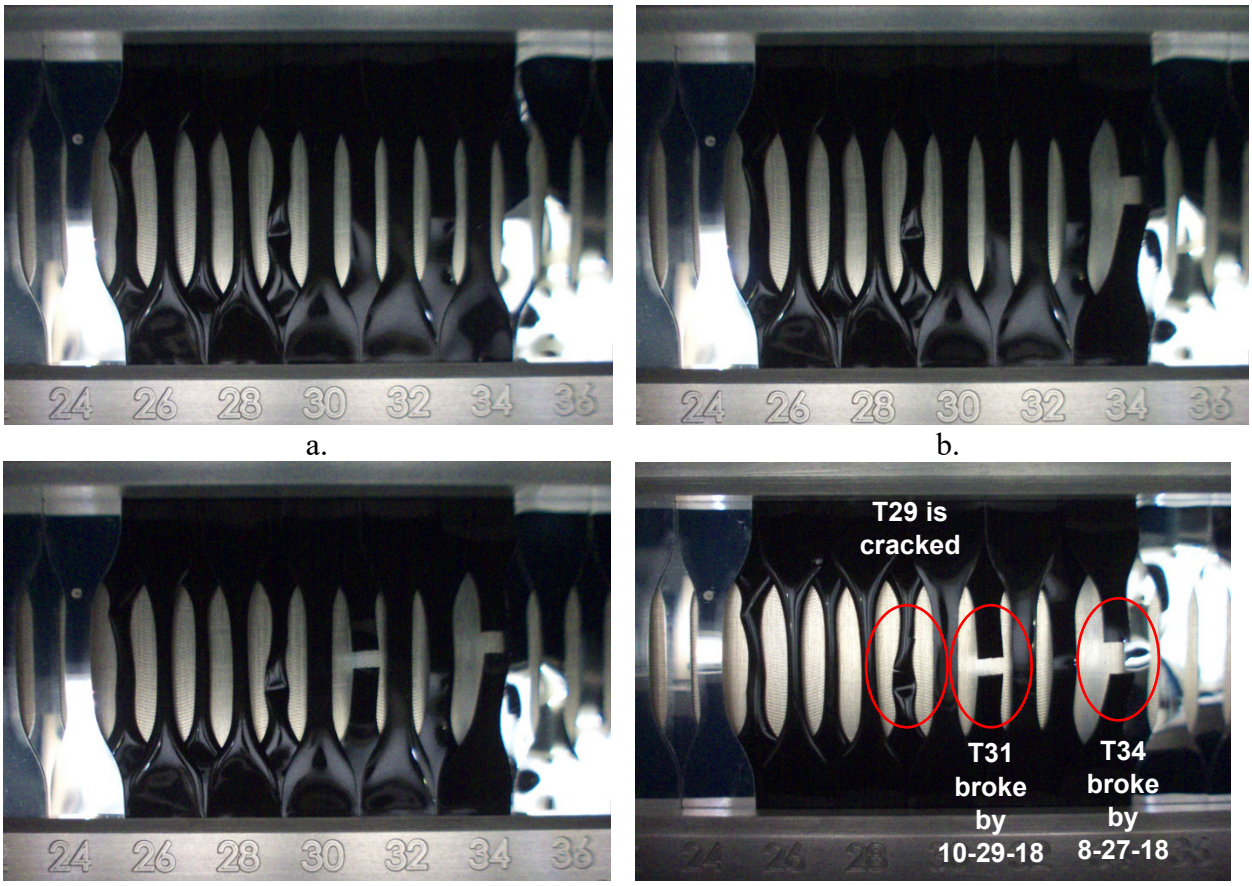


Figure 24. On-orbit photographs of the MISSE-9 PCE-1 wake C-FEP samples: a). Image taken on July 25, 2018, b). Image taken on August 27, 2018, c). Image taken on October 29, 2018, and d). Image taken December 26, 2018.

*Post-Flight Photographs*

Figure 25 provides a post-flight photograph of the 38 MISSE-9 PCE-1 wake tensile samples in the MSC deck. As can be seen, all the metallized Teflon FEP samples (Al-FEP and Ag-FEP) are intact. In addition, the two broken C-FEP samples (M9W-T31 and M9W-T34) are visible. Figure 26 provides a post-flight photograph of the MISSE-9 PCE-1 zenith tensile samples in the MSC deck. All samples, including the C-FEP samples, are intact.

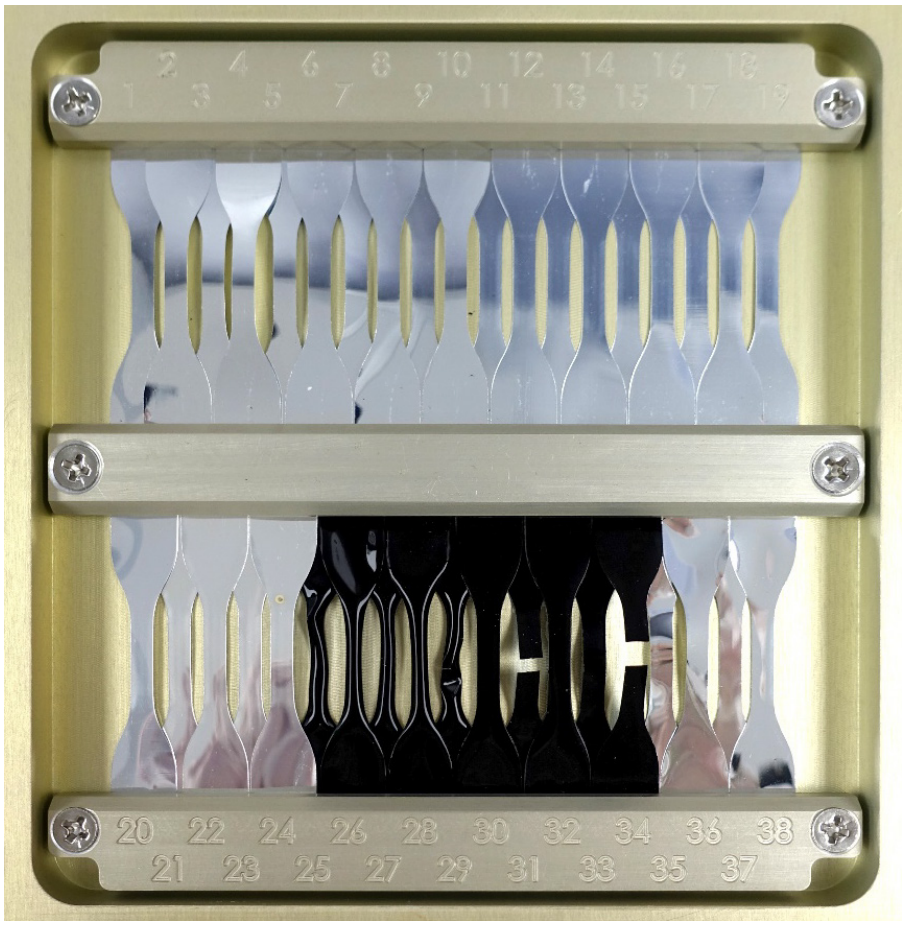


Figure 25. Post-flight photograph of the MISSE-9 PCE-1 wake tensile samples.


Figure 26. Post-flight photograph of the MISSE-9 PCE-1 zenith tensile samples.

*Thickness Measurements*

Tables 10 and 11 provides the average thickness measurements for the MISSE-9 PCE-1 wake and zenith tensile samples, respectively. These tables provide the MISSE ID, number of samples, material, flight or control sample, average thicknesses, standard deviation of thicknesses, and percent change in thickness of the flight samples as compared to the control samples. It should be noted that the C-FEP sample thickness has more variability from sample to sample due to the coating application. There does not appear to be any obvious trends for thickness loss for either the wake or zenith samples. This is not surprising due to the very low AO exposure and relatively low mission exposure for these samples.

Table 10. Thickness Data for the MISSE-9 PCE-1 Wake Tensile Samples.

| MISSE Sample ID | # of Samples | Material | Flight or Control | AVG Thickness (mils) | Std. Dev. (mils) | Flight vs. Control Thickness (% Change) |
|---|---|---|---|---|---|---|
| M9W-T1 to T5 F | 5 | 2 mil Al-FEP (P) | Flight | 1.97 | 0.03 | 3.1 |
| M9W-T1 to T5 C | 5 | | Control | 1.91 | 0.01 | |
| M9W-T6 to T10 F | 5 | 2 mil Al-FEP (N) | Flight | 1.96 | 0.02 | -0.6 |
| M9W-T6 to T10 C | 5 | | Control | 1.97 | 0.02 | |
| M9W-T11 to T15 F | 5 | 5 mil Al-FEP (P) | Flight | 4.49 | 0.02 | -0.1 |
| M9W-T11 to T14 C | 4 | | Control | 4.49 | 0.09 | |
| M9W-T16 to T20 F | 5 | 5 mil Al-FEP (N) | Flight | 4.50 | 0.08 | 0.4 |
| M9W-T16 to T19 C | 4 | | Control | 4.48 | 0.04 | |
| M9W-T21 to T24 F | 4 | 5 mil Ag-FEP (P) | Flight | 4.51 | 0.15 | -0.3 |
| M9W-T21 to T24.1 C | 5 | | Control | 4.52 | 0.14 | |
| M9W-T25 to T29 F | 5 | 2 mil C-FEP (P) | Flight | 2.35 | 0.16 | -5.4 |
| M9W-T25 to T29 C | 5 | | Control | 2.49 | 0.36 | |
| M9W-T30 to T34 F | 5 | 5 mil C-FEP (P) | Flight | 5.43 | 0.20 | 2.8 |
| M9W-T30 to T34 C | 5 | | Control | 5.29 | 0.18 | |
| M9W-T35 to T38 F | 4 | 2 mil Al/FEP (P) | Flight | 1.91 | 0.02 | -0.5 |
| M9W-T35 to T38.1 C | 5 | | Control | 1.92 | 0.03 | |

Table 11. Thickness Data for the MISSE-9 PCE-1 Zenith Tensile Samples.

| MISSE Sample ID | # of Samples | Material | Flight or Control | AVG Thickness (mils) | Std. Dev. (mils) | Flight vs. Control Thickness (% Change) |
|---|---|---|---|---|---|---|
| M9Z-T1 to T4 F | 4 | 2 mil Al-FEP (P) | Flight | 1.98 | 0.06 | -0.2 |
| M9Z-T1 to T3 C | 3 | | Control | 1.98 | 0.06 | |
| M9Z-T5 to T8 F | 4 | 2 mil Al-FEP (N) | Flight | 1.95 | 0.01 | 0.2 |
| M9Z-T5 to T7 C | 3 | | Control | 1.95 | 0.01 | |
| M9Z-T9 to T12 F | 4 | 5 mil Al-FEP (P) | Flight | 4.54 | 0.04 | -0.8 |
| M9Z-T9 to T11 C | 3 | | Control | 4.57 | 0.03 | |
| M9Z-T13 to T16 F | 4 | 5 mil Al-FEP (N) | Flight | 4.52 | 0.05 | 0.5 |
| M9Z-T13 to T16 C | 4 | | Control | 4.49 | 0.06 | |
| M9Z-T17 to T20 F | 4 | 2 mil C-FEP (P) | Flight | 2.52 | 0.17 | 8.0 |
| M9Z-T17 & T18 C | 2 | | Control | 2.33 | 0.08 | |
| M9Z-T21 to T24 F | 4 | 2 mil Al/FEP (P) | Flight | 1.94 | 0.05 | 0.4 |
| M9Z-T21 & T22 C | 2 | | Control | 1.93 | 0.01 | |

*Tensile Results*

The MISSE-9 PCE-1 wake and zenith sample tensile data is provided in Table 12 and Table 13, respectively. The tables include the tensile sample IDs, whether it is a flight (F) or control (C) sample, material, nominal film thickness, elastic modulus, yield strength, ultimate tensile strength (UTS), average UTS with standard deviation, percent change in average flight UTS as compared to the control, %E, average %E with standard deviation, and the percent change in average flight %E as compared to the control.

Table 12. Tensile Data for the MISSE-9 PCE-1 Wake Tensile Samples.

| MISSE-9 Wake ID | Flight or Control | Material | Nominal Thickness (inch) | Elastic Modulus (MPa) | Yield Strength (MPa) | UTS (MPa) | Ave. UTS (MPa) | Percent Change in UTS | % Elong. (%E) | Ave. %E | Percent Change in %E |
|---|---|---|---|---|---|---|---|---|---|---|---|
| M9W-T1 | F | Al-FEP (P) | 0.002 | 720.27 | 12.30 | 23.86 | 23.032 ± 1.02 | -34.46 | **186.23** | 176.84 ± 13.21 | -31.05 |
| M9W-T2 | F | | | 718.77 | 12.39 | 23.45 | | | **183.22** | | |
| M9W-T3 | F | | | 691.36 | 12.43 | 22.41 | | | **177.98** | | |
| M9W-T4 | F | | | 720.63 | 12.71 | 21.56 | | | **153.81** | | |
| M9W-T5 | F | | | 725.48 | 12.64 | 23.88 | | | **182.97** | | |
| M9W-T1 | C | Al-FEP (P) | 0.002 | 698.72 | 12.32 | 35.80 | 35.144 ± 2.89 | | **263.12** | 256.46 ± 20.43 | |
| M9W-T2 | C | | | 699.92 | 12.29 | 36.23 | | | **265.35** | | |
| M9W-T3 | C | | | 691.88 | 12.13 | 35.00 | | | **259.88** | | |
| M9W-T4 | C | | | 696.72 | 12.33 | 38.25 | | | **273.01** | | |
| M9W-T5 | C | | | 689.03 | 12.49 | 30.44 | | | **220.96** | | |
| M9W-T6 | F | Al-FEP (N) | 0.002 | 714.85 | 12.13 | 15.40 | 16.11 ± 0.72 | -42.67 | **144.29** | 155.47 ± 15.78 | -48.66 |
| M9W-T7 | F | | | 708.97 | 12.30 | 17.20 | | | **180.83** | | |
| M9W-T8 | F | | | 727.82 | 12.28 | 15.75 | | | **154.75** | | |
| M9W-T9 | F | | | 730.88 | 12.45 | 16.45 | | | **157.00** | | |
| M9W-T10 | F | | | 753.08 | 12.77 | 15.76 | | | **140.47** | | |
| M9W-T6 | C | Al-FEP (N) | 0.002 | 695.55 | 12.13 | 25.82 | 28.10 ± 1.41 | | **277.22** | 302.82 ± 18.38 | |
| M9W-T7 | C | | | 689.56 | 11.82 | 29.52 | | | **324.12** | | |
| M9W-T8 | C | | | 688.10 | 11.91 | 28.69 | | | **315.60** | | |
| M9W-T9 | C | | | 708.15 | 12.26 | 27.82 | | | **293.96** | | |
| M9W-T10 | C | | | 708.73 | 12.27 | 28.66 | | | **303.20** | | |
| M9W-T11 | F | Al-FEP (P) | 0.005 | 652.65 | 11.86 | 17.93 | 16.622 ± 1.06 | -37.60 | **188.13** | 159.73 ± 20.16 | -46.89 |
| M9W-T12 | F | | | 653.04 | 11.81 | 15.75 | | | **145.61** | | |
| M9W-T13 | F | | | 650.52 | 11.76 | 15.49 | | | **140.01** | | |
| M9W-T14 | F | | | 673.59 | 12.12 | 16.49 | | | **152.06** | | |
| M9W-T15 | F | | | 670.50 | 12.19 | 17.45 | | | **172.84** | | |
| M9W-T11 | C | Al-FEP (P) | 0.005 | 646.46 | 11.77 | 25.89 | 26.6375 ± 0.56 | | **294.68** | 300.73 ± 4.43 | |
| M9W-T12 | C | | | 633.68 | 11.68 | 26.54 | | | **304.22** | | |
| M9W-T13 | C | | | 655.64 | 11.89 | 27.00 | | | **300.15** | | |
| M9W-T14 | C | | | 651.27 | 11.81 | 27.12 | | | **303.86** | | |
| M9W-T16 | F | Al-FEP (N) | 0.005 | 632.11 | 11.46 | 15.37 | 16.16 ± 1.05 | -34.33 | **124.36** | 141.63 ± 18.73 | -47.03 |
| M9W-T17 | F | | | 619.47 | 11.59 | 15.32 | | | **128.60** | | |
| M9W-T18 | F | | | 635.70 | 11.51 | 16.05 | | | **148.17** | | |
| M9W-T19 | F | | | 657.33 | 11.90 | 17.91 | | | **170.97** | | |
| M9W-T20 | F | | | 656.84 | 11.94 | 16.15 | | | **136.07** | | |
| M9W-T16 | C | Al-FEP (N) | 0.005 | 621.47 | 11.51 | 21.36 | 24.6075 ± 2.26 | | **227.45** | 267.40 ± 28.98 | |
| M9W-T17 | C | | | 610.25 | 11.23 | 25.98 | | | **293.35** | | |
| M9W-T18 | C | | | 633.35 | 11.69 | 24.81 | | | **265.66** | | |
| M9W-T19 | C | | | 639.76 | 11.55 | 26.28 | | | **283.12** | | |

Table 12. Tensile Data for the MISSE-9 PCE-1 Wake Tensile Samples.

| MISSE-9 Wake ID | Flight or Control | Material | Nominal Thickness (inch) | Elastic Modulus (MPa) | Yield Strength (MPa) | UTS (MPa) | Ave. UTS (MPa) | Percent Change in UTS | % Elong. (%E) | Ave. %E | Percent Change in %E |
|---|---|---|---|---|---|---|---|---|---|---|---|
| M9W-T21 | F | Ag-FEP (P) | 0.005 | 684.12 | 11.56 | 15.73 | 16.33 ± 1.64 | -36.03 | **156.84** | 158.04 ± 32.91 | -47.28 |
| M9W-T22 | F | | | 687.27 | 11.59 | 14.81 | | | **123.02** | | |
| M9W-T23 | F | | | 699.50 | 11.95 | 16.14 | | | **150.03** | | |
| M9W-T24 | F | | | 710.11 | 11.77 | 18.64 | | | **202.28** | | |
| M9W-T21 | C | Ag-FEP (P) | 0.005 | 675.23 | 11.65 | 24.67 | 25.526 ± 0.93 | | **292.10** | 299.76 ± 8.24 | |
| M9W-T22 | C | | | 689.24 | 11.40 | 25.52 | | | **303.01** | | |
| M9W-T23 | C | | | 683.28 | 11.63 | 24.61 | | | **291.84** | | |
| M9W-T24 | C | | | 700.52 | 11.97 | 26.81 | | | **311.56** | | |
| M9W-T24.1 | C | | | 703.29 | 11.75 | 26.02 | | | **300.30** | | |
| M9W-T25 | F | C-FEP (P) | 0.002 | 512.27 | 14.12 | 16.88 | 15.544 ± 5.89 | -41.64 | **17.11** | 14.26 ± 8.62 | -94.61 |
| M9W-T26 | F | | | 830.12 | 17.31 | 21.21 | | | **18.38** | | |
| M9W-T27 | F | | | 681.78 | 16.20 | 17.89 | | | **9.44** | | |
| M9W-T28 | F | | | 737.74 | 15.19 | 16.14 | | | **24.30** | | |
| M9W-T29 | F | | | 350.61 | 5.43 | 5.60 | | | **2.09** | | |
| M9W-T25 | C | C-FEP (P) | 0.002 | 481.47 | 10.51 | 28.18 | 26.636 ± 2.50 | | **296.39** | 264.68 ± 43.17 | |
| M9W-T26 | C | | | 471.22 | 10.37 | 28.93 | | | **305.92** | | |
| M9W-T27 | C | | | 437.20 | 10.12 | 27.28 | | | **284.82** | | |
| M9W-T28 | C | | | 562.32 | 11.01 | 26.24 | | | **220.50** | | |
| M9W-T29 | C | | | 281.78 | 21.31 | 22.55 | | | **215.78** | | |
| M9W-T30 | F | C-FEP (P) | 0.005 | 789.45 | 12.55 | 15.73 | 15.63 ± 0.09 | -40.04 | **33.11** | 27.18 ± 5.57 | -90.63 |
| M9W-T32** | F | | | 796.25 | 12.70 | 15.59 | | | **26.36** | | |
| M9W-T33** | F | | | 842.80 | 12.97 | 15.57 | | | **22.06** | | |
| M9W-T30 | C | C-FEP (P) | 0.005 | 506.56 | 10.55 | 25.22 | 26.068 ± 0.63 | | **280.66** | 289.95 ± 7.39 | |
| M9W-T31 | C | | | 558.30 | 11.18 | 26.02 | | | **287.25** | | |
| M9W-T32 | C | | | 542.02 | 10.94 | 26.82 | | | **301.07** | | |
| M9W-T33 | C | | | 521.25 | 10.73 | 25.76 | | | **289.65** | | |
| M9W-T34 | C | | | 573.62 | 11.16 | 26.52 | | | **291.11** | | |
| M9W-T35 | F | Al/FEP (P) | 0.002 | 677.17 | 12.52 | 28.29 | 27.2575 ± 4.82 | -22.43 | **200.72** | 193.50 ± 43.40 | -22.52 |
| M9W-T36 | F | | | 694.76 | 12.54 | 30.72 | | | **220.38** | | |
| M9W-T37 | F | | | 705.88 | 12.38 | 20.19 | | | **130.11** | | |
| M9W-T38 | F | | | 692.37 | 12.34 | 29.83 | | | **222.79** | | |
| M9W-T35 | C | Al/FEP (P) | 0.002 | 717.67 | 12.78 | 34.77 | 35.138 ± 1.54 | | **242.43** | 249.73 ± 12.69 | |
| M9W-T36 | C | | | 689.87 | 12.68 | 32.66 | | | **230.75** | | |
| M9W-T37 | C | | | 697.81 | 12.90 | 36.66 | | | **258.66** | | |
| M9W-T38 | C | | | 692.46 | 12.27 | 35.72 | | | **258.24** | | |
| M9W-T38.1 | C | | | 709.91 | 12.56 | 35.88 | | | **258.56** | | |

*FEP layer is space facing for all samples except Al/FEP

****M9W-T31 F and M9W-T34 F broke on-orbit**

Table 13. Tensile Data for the MISSE-9 PCE-1 Zenith Tensile Samples.

| MISSE-9 Zenith ID | Flight or Control | Material | Nominal Thickness (inch) | Elastic Modulus (MPa) | Yield Strength (MPa) | UTS (MPa) | Ave. UTS (MPa) | Percent Change in UTS | % Elong. (%E) | Ave. %E | Percent Change in %E |
|---|---|---|---|---|---|---|---|---|---|---|---|
| M9Z-T1 | F | Al-FEP (P) | 0.002 | 723.34 | 12.98 | 19.52 | 19.25 ± 0.97 | -48.9 | **130.60** | 125.30 ± 15.84 | -53.1 |
| M9Z-T2 | F | | | 717.27 | 12.89 | 19.67 | | | **129.86** | | |
| M9Z-T3 | F | | | 727.32 | 12.67 | 19.98 | | | **138.47** | | |
| M9Z-T4 | F | | | 715.31 | 12.41 | 17.82 | | | **102.26** | | |
| M9Z-T1 | C | Al-FEP (P) | 0.002 | 688.75 | 12.84 | 39.91 | 37.63 ± 2.26 | | **282.36** | 267.15 ± 16.11 | |
| M9Z-T2 | C | | | 677.51 | 12.50 | 35.39 | | | **250.27** | | |
| M9Z-T3 | C | | | 704.56 | 12.54 | 37.59 | | | **268.82** | | |
| M9Z-T5 | F | Al-FEP (N) | 0.002 | 725.16 | 12.61 | 14.98 | 14.85 ± 0.25 | -50.3 | **77.31** | 78.27 ± 2.71 | -74.5 |
| M9Z-T6 | F | | | 719.85 | 12.80 | 15.11 | | | **79.75** | | |
| M9Z-T7 | F | | | 730.36 | 12.47 | 14.53 | | | **74.95** | | |
| M9Z-T8 | F | | | 724.10 | 12.46 | 14.77 | | | **81.07** | | |
| M9Z-T5 | C | Al-FEP (N) | 0.002 | 698.85 | 12.73 | 30.69 | 29.86 ± 1.27 | | **313.60** | 307.40 ± 15.92 | |
| M9Z-T6 | C | | | 707.90 | 12.55 | 28.39 | | | **289.31** | | |
| M9Z-T7 | C | | | 718.28 | 12.25 | 30.49 | | | **319.28** | | |
| M9Z-T9 | F | Al-FEP (P) | 0.005 | 681.15 | 12.27 | 15.27 | 14.93 ± 0.28 | -47.2 | **110.53** | 101.44 ± 7.15 | -67.4 |
| M9Z-T10 | F | | | 676.84 | 12.31 | 15.06 | | | **95.35** | | |
| M9Z-T11 | F | | | 668.39 | 12.00 | 14.67 | | | **96.12** | | |
| M9Z-T12 | F | | | 654.34 | 12.08 | 14.73 | | | **103.77** | | |
| M9Z-T9 | C | Al-FEP (P) | 0.005 | 668.46 | 12.10 | 28.23 | 28.30 ± 0.85 | | **309.93** | 311.09 ± 5.80 | |
| M9Z-T10 | C | | | 669.79 | 12.12 | 29.19 | | | **317.38** | | |
| M9Z-T11 | C | | | 660.39 | 11.96 | 27.49 | | | **305.96** | | |
| M9Z-T13 | F | Al-FEP (N) | 0.005 | 664.70 | 12.01 | 15.29 | 15.00 ± 0.22 | -43.7 | **92.81** | 83.93 ± 9.05 | -70.6 |
| M9Z-T14 | F | | | 655.37 | 11.97 | 14.94 | | | **72.14** | | |
| M9Z-T15 | F | | | 657.34 | 11.82 | 15.01 | | | **81.96** | | |
| M9Z-T16 | F | | | 643.34 | 11.74 | 14.77 | | | **88.81** | | |
| M9Z-T13 | C | Al-FEP (N) | 0.005 | 645.74 | 11.96 | 26.52 | 26.66 ± 1.02 | | **281.02** | 285.59 ± 12.92 | |
| M9Z-T14 | C | | | 636.00 | 11.67 | 26.97 | | | **290.13** | | |
| M9Z-T15 | C | | | 631.01 | 11.65 | 25.36 | | | **270.44** | | |
| M9Z-T16 | C | | | 647.80 | 11.80 | 27.80 | | | **300.75** | | |
| M9Z-T17 | F | C-FEP (P) | 0.002 | 910.02 | 14.83 | 16.54 | 17.78 ± 1.77 | -36.7 | **16.46** | 8.515 ± 5.79 | -96.2 |
| M9Z-T18 | F | | | 629.50 | 15.67 | 18.16 | | | **9.09** | | |
| M9Z-T19 | F | | | 868.81 | 15.28 | 16.28 | | | **4.92** | | |
| M9Z-T20 | F | | | 788.84 | 19.79 | 20.12 | | | **3.59** | | |
| M9Z-T17 | C | C-FEP (P) | 0.002 | 504.08 | 10.60 | 28.94 | 28.10 ± 1.20 | | **234.26** | 227.03 ± 10.23 | |
| M9Z-T18 | C | | | 538.51 | 10.89 | 27.25 | | | **219.79** | | |

Table 13. Tensile Data for the MISSE-9 PCE-1 Zenith Tensile Samples.

| MISSE-9 Zenith ID | Flight or Control | Material | Nominal Thickness (inch) | Elastic Modulus (MPa) | Yield Strength (MPa) | UTS (MPa) | Ave. UTS (MPa) | Percent Change in UTS | % Elong. (%E) | Ave. %E | Percent Change in %E |
|---|---|---|---|---|---|---|---|---|---|---|---|
| M9Z-T21 | F | Al/FEP (P) | 0.002 | 700.17 | 12.72 | 23.40 | 25.02 ± 1.35 | -31.4 | **165.64** | 180.85 ± 11.83 | -31.8 |
| M9Z-T22 | F | | | 677.09 | 12.54 | 26.69 | | | **194.53** | | |
| M9Z-T23 | F | | | 712.61 | 12.56 | 24.86 | | | **181.42** | | |
| M9Z-T24 | F | | | 695.92 | 12.62 | 25.12 | | | **181.82** | | |
| M9Z-T21 | C | Al/FEP (P) | 0.002 | 702.04 | 12.48 | 38.31 | 36.45 ± 2.63 | | **274.29** | 265.18 ± 12.89 | |
| M9Z-T22 | C | | | 676.53 | 12.23 | 34.59 | | | **256.06** | | |

*FEP layer is space facing for all samples except Al/FEP

Figure 27 is a bar chart showing the average %E values, with standard deviation error bars, for the MISSE-9 PCE-1 Teflon FEP wake flight and control tensile samples. The Teflon FEP samples were significantly embrittled after only 0.54 years of wake space exposure. The 2 mil Al-FEP "normal (N)" samples had a larger decrease in %E (48.7%) than the 2 mil Al-FEP "parallel (P)" samples (31.1%). However, the extent of embrittlement for the 5 mil FEP samples was not impacted by the die-cut direction (≈47% change in %E for all 5 mil FEP samples).

Aluminized Teflon samples with the aluminized side facing space (Al/FEP) were slightly less embrittled than samples with the FEP facing space (FEP/Al). The Al/FEP samples had an average 193.50 %E, compared to 141.63-176.84 %E for the FEP/Al samples. Thus, the 1000 Å Al film provided some protection to the Teflon, but deeper penetrating radiation still caused embrittlement.

By far, the most embrittled samples were those with the carbon coating. As stated previously, two of the 5 mil C-FEP wake samples (M9W-T31 F and M9W-T34 F) broke on-orbit. Both the 2 mil C-FEP and 5 mil C-FEP samples were severely embrittled with the thinner 2 mil C-FEP being more embrittled (14.26 ± 8.62 %E) than the thickener 5 mil C-FEP (27.18 ± 5.57 %E).

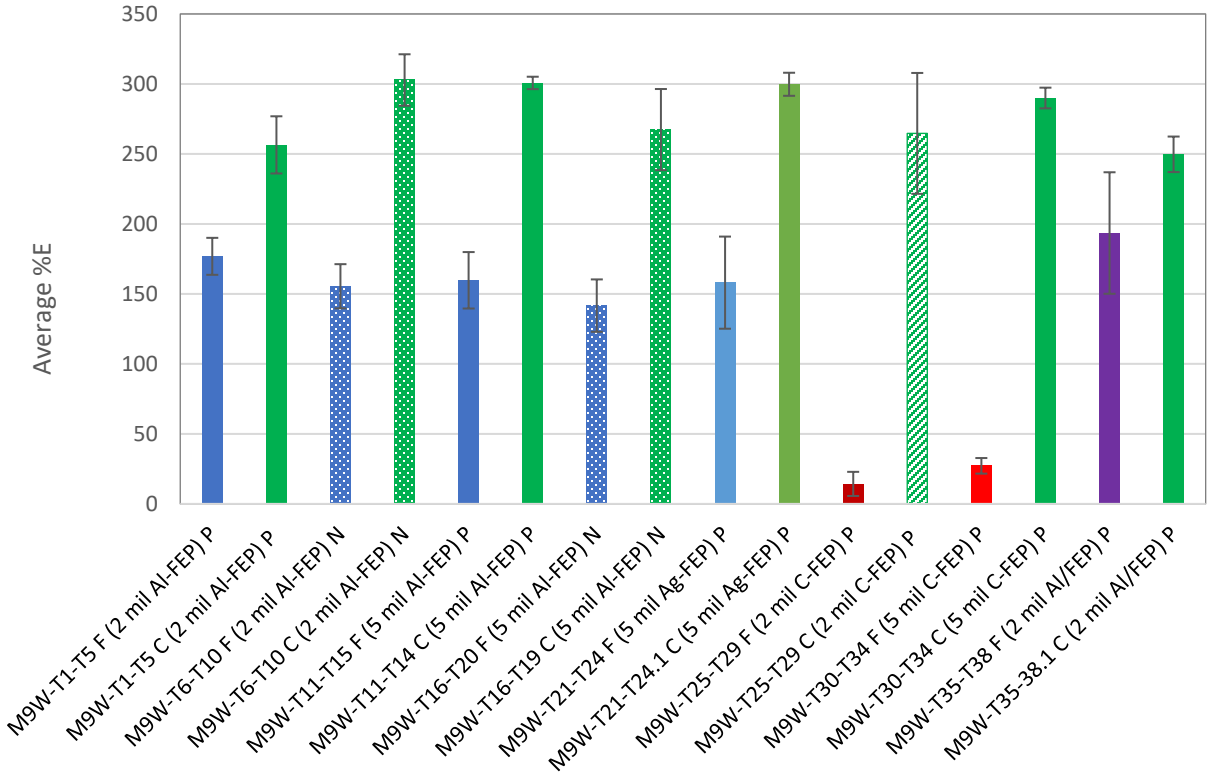


Figure 27. Bar chart showing the average %E for the MISSE-9 PCE-1 wake Teflon FEP flight (F) and control (C, green) samples.

Figure 28 is a bar chart showing the average %E values, with standard deviation error bars, for the MISSE-9 PCE-1 Teflon FEP zenith flight and control tensile samples. The zenith sample trends are similar to the wake sample trends but with more embrittlement overall. Like the wake samples, the Teflon FEP zenith samples were significantly embrittled after only 0.54 years of zenith space exposure. Also, like the wake samples, the 2 mil Al-FEP normal (N) samples had a larger decrease in %E (74.5%) than the 2 mil Al-FEP parallel (P) samples (53.1%). And again, the extent of embrittlement for the 5 mil samples was not impacted by the die-cut direction (67.4% decrease in %E for the N samples and 70.6% decrease for the P samples). Also like the wake samples, there was embrittlement in the 2 mil Al/FEP samples with the aluminum side facing space, but with less embrittlement than the 2 mil Al-FEP samples with the Teflon side facing space. The aluminum facing Al/FEP samples had an average 180.85 %E as compared to 78.3-125.3 %E for the space facing FEP samples. This data further indicates that the aluminized layer provided some protection, but damaging space radiation penetrates through the 1000 Å Al layer. And, once again, the 2 mil C-FEP samples were severely embrittled with only 8.52 ± 5.79 %E, a decrease of 96.2% as compared to the control samples.

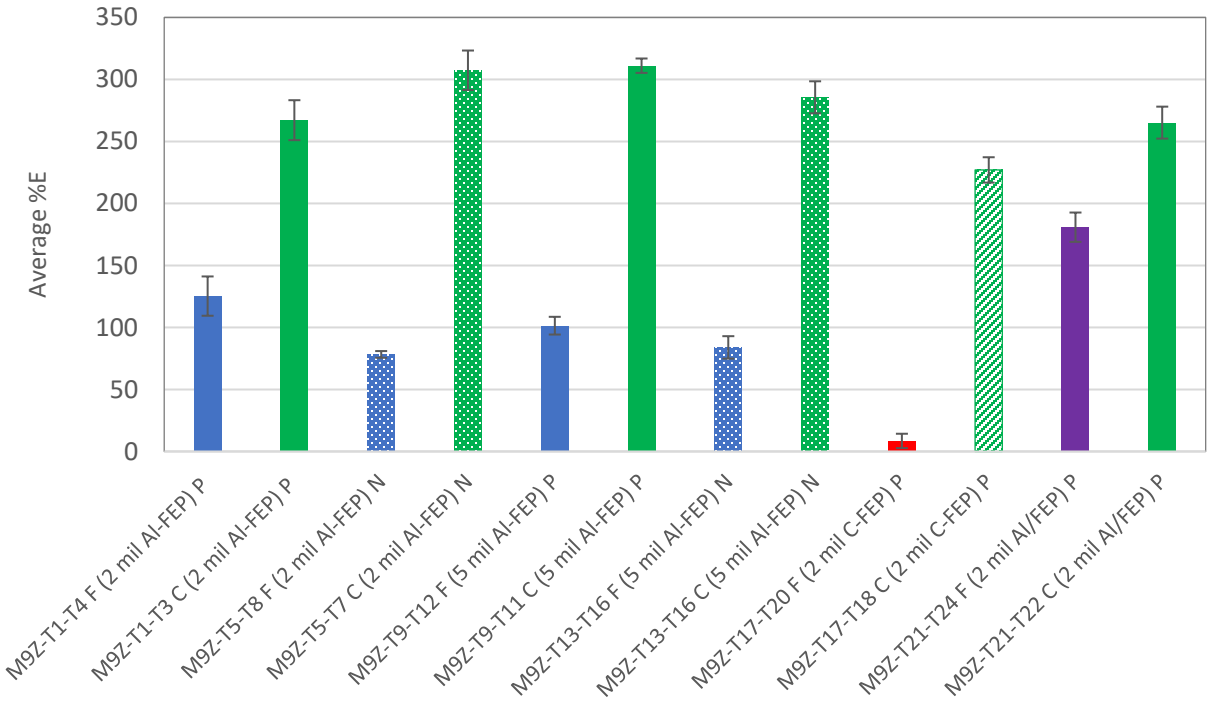


Figure 28. Bar chart showing the average %E for the MISSE-9 PCE-1 zenith (M9Z) Teflon FEP flight (F) and control (C, green) samples.

Figure 29 provides a bar chart comparing the average %E for the MISSE-9 PCE-1 wake (M9W) and zenith (M9Z) P and N Al-FEP and Ag-FEP flight and control samples so trends in the die-cut direction can be made for all samples. The control averages provided in Figure 29 include all control samples values for similar materials (wake and zenith). As mentioned previously, the 2 mil Al-FEP N control samples have a higher %E (304.5 %E) than the 2 mil Al-FEP P samples (260.5 %E). But, the 5 mil Al-FEP and Ag-FEP samples do not seem to be as affected by sectioning with respect to the roll direction with the 5 mil Al-FEP N having a 276.5 %E, the 5 mil Al-FEP P having a somewhat higher 305.2 %E, and the 5 mil Ag-FEP P having a 299.8 %E. When comparing the wake and zenith data side-by-side in Figure 29, it becomes apparent that the zenith samples are consistently more embrittled then the wake samples for similar direct space exposure durations.

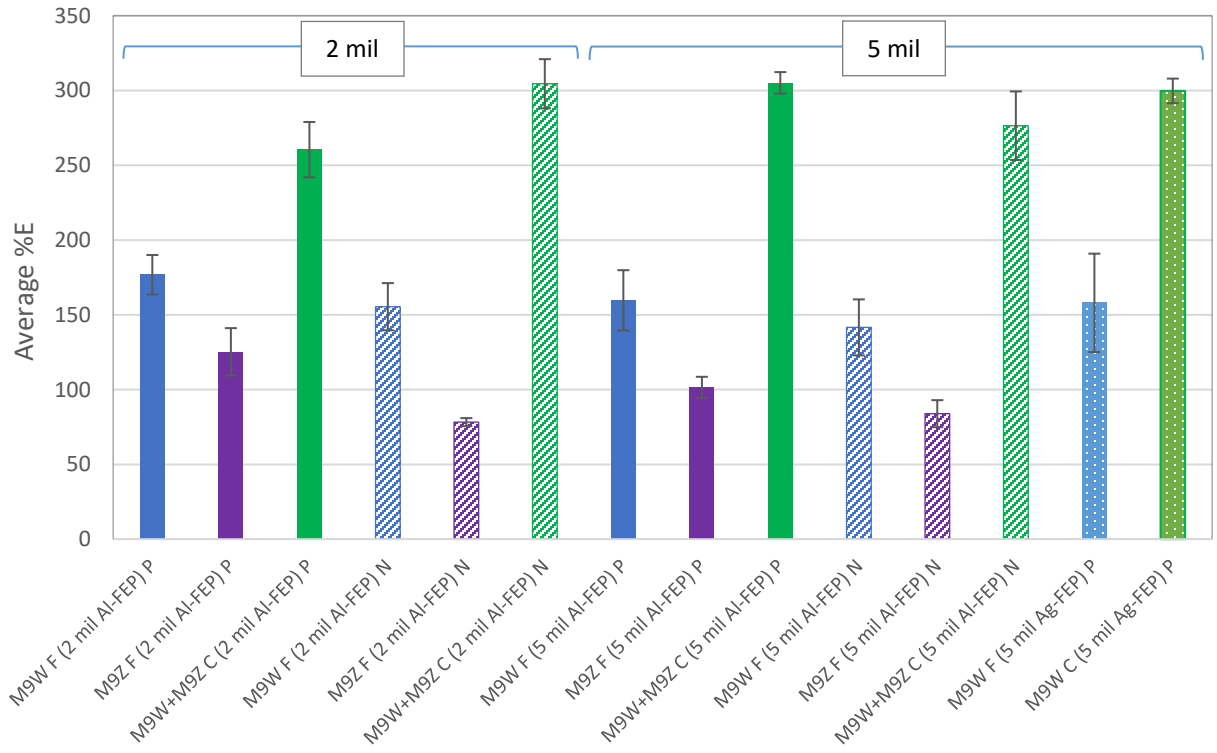


Figure 29. Bar chart comparing the average %E for the MISSE-9 PCE-1 wake (M9W) and zenith (M9Z) flight and control tensile samples.

Figure 30 is a bar chart with the average %E for all MISSE-9 PCE-1 wake and zenith Teflon "parallel" to the roll direction (P) Teflon FEP samples. Again, the zenith tensile samples are consistently more embrittled than the wake samples for the same type of material and the same space exposure durations (1.07 years of vacuum space exposure and 0.54 years of direct wake or zenith space exposure). Again, this chart shows that the 2 mil C-FEP and 5 mil C-FEP samples were severely embrittled. As previously discussed, prior ground-test and flight data indicates that Teflon FEP embrittlement is caused by radiation exposure, and the level of embrittlement is increased with higher thermal exposures.[6,24-26] The AO fluence was a little higher for the zenith samples (3.19 x $10^{18}$ atoms/cm$^2$) than the wake samples (4.46 x $10^{16}$ atoms/cm$^2$), as indicated in Table 5, but there were no consistent thickness loss trends for the zenith samples. So, although a

high AO exposure can remove a UV radiation surface embrittled layer, it is not likely the AO exposure had a significant impact on the resulting embrittlement due to the very low AO fluence levels.

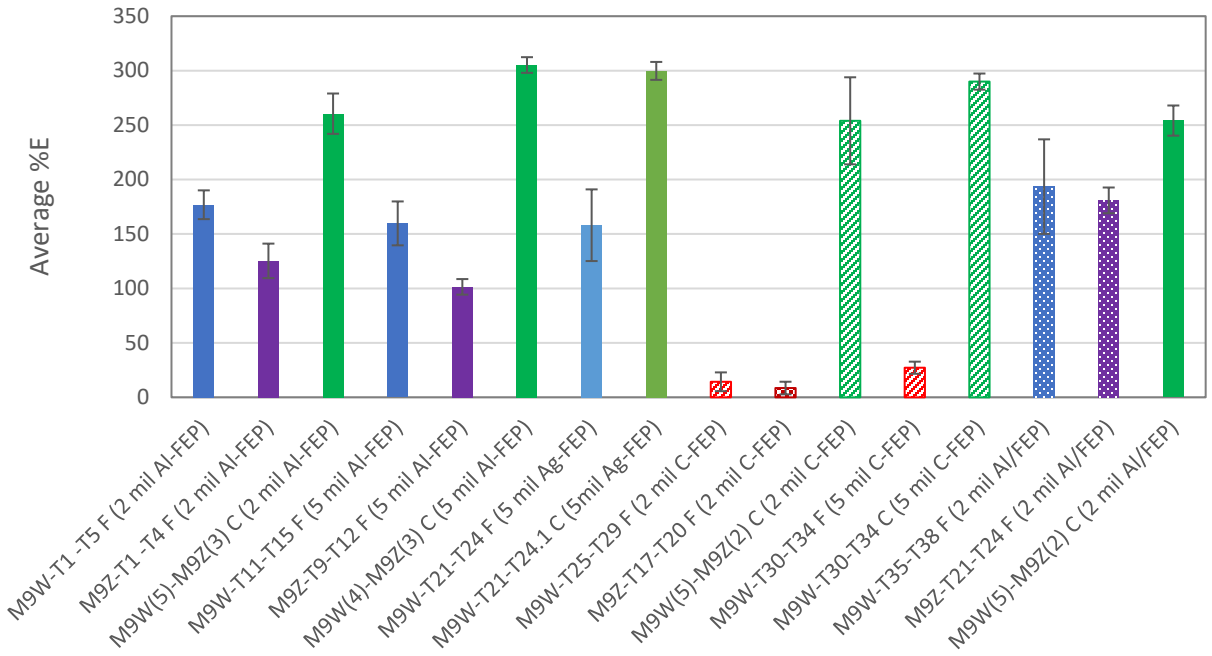


Figure 30. Bar chart showing the average %E for all MISSE-9 PCE-1 wake and zenith Teflon parallel (P) flight (F) and control (C, green) samples.

### *MISSE-13 Polymers and Composites Experiment-4 (PCE-4)*

*Post-Flight Photographs*

Figure 31 provides post-flight photographs of the 24 MISSE-13 PCE-4 wake tensile samples in the flight holder and during the de-integration process (i.e. removal from flight hardware). As can be seen, all samples returned intact and the amber colored Kapton support on one of the gossamer thin solar sail samples is visible.


a.

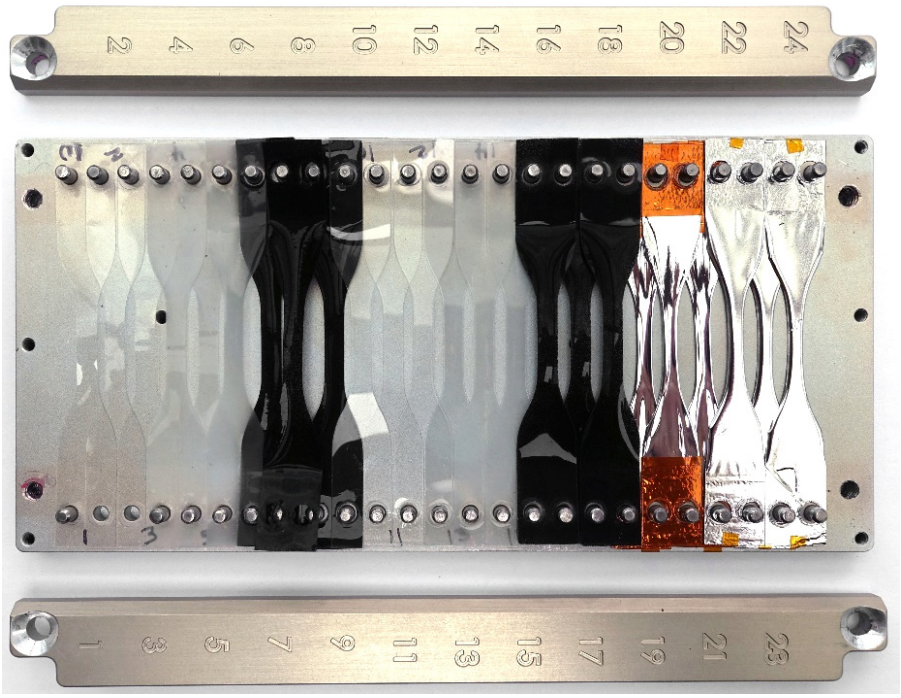

b.

Figure 31. Post-flight photographs of the MISSE-13 PCE-4 wake tensile samples, a). Samples loaded in flight hardware, and b). During the sample de-integration process.

*Thickness Measurements*

Table 14 provides the average thickness measurements for the MISSE-13 PCE-4 wake tensile samples. The table provides the MISSE ID, number of samples, material, flight or control sample, average thicknesses, standard deviation of thicknesses, and percent change in thickness of the flight samples as compared to the control samples. It should be noted that there is a larger variability in the thickness of FEP-AO and C-FEP due to the AO treatment (FEP-AO) or the combined AO and carbon coating application (C-FEP). Although the 2 mil and 5 mil FEP flight samples both experience some thickness loss, there are not any obvious trends for thickness loss for the samples. Again, this is not surprising due to the very low AO fluence for samples facing the wake direction and relatively low total mission exposure duration for these samples.

Table 14. Thickness Data for the MISSE-13 PCE-4 Wake Tensile Samples.

| MISSE Sample ID | # of Samples | Material | Flight or Control | AVG Thickness (mils) | Std. Dev. (mils) | Flight vs. Control Thickness (% Change) |
|---|---|---|---|---|---|---|
| M13W-T1 to T3 F | 3 | 2 mil FEP (P) | Flight | 1.83 | 0.05 | -0.4 |
| M13W-T1 to T3.2 C | 5 | | Control | 1.84 | 0.04 | |
| M13W-T4 to T6 F | 3 | 2 mil FEP-AO (P) | Flight | 1.58 | 0.02 | 6.4 |
| M13W-T4 to T6.2 C | 5 | | Control | 1.48 | 0.08 | |
| M13W-T7 to T9 F | 3 | 2 mil C-FEP (P) | Flight | 2.08 | 0.01 | 1.1 |
| M13W-T7 to T9.2 C | 5 | | Control | 2.06 | 0.03 | |
| M13W-T10 to T12 F | 3 | 5 mil FEP (P) | Flight | 4.82 | 0.11 | -0.9 |
| M13W-T10 to T12.2 C | 5 | | Control | 4.87 | 0.12 | |
| M13W-T13 to T15 F | 3 | 5 mil FEP-AO (P) | Flight | 4.55 | 0.11 | -0.8 |
| M13W-T13 to T15.2 C | 5 | | Control | 4.58 | 0.10 | |
| M13W-T16 to T18 F | 3 | 5 mil C-FEP (P) | Flight | 5.12 | 0.11 | 3.3 |
| M13W-T16 to T18.2 C | 5 | | Control | 4.95 | 0.06 | |
| M13W-T19 to T21 F | 3 | 0.2 mil VDA/CP1 | Flight | 0.24 | 0.01 | 0.0 |
| M13W-T19 to T21.2 C | 5 | | Control | 0.24 | 0.00 | |
| M13W-T22 to T24 F | 3 | 0.3 mil VDA/CP1-PTFE | Flight | 0.34 | 0.03 | 6.8 |
| M13W-T22 to T24.2 C | 5 | | Control | 0.31 | 0.03 | |

*Tensile Results*

The MISSE-13 PCE-4 wake sample tensile data is provided in Table 15. The table includes the tensile sample IDs, whether it is a flight (F) or control (C) sample, material, nominal film thickness, elastic modulus, yield strength, ultimate tensile strength (UTS), average UTS with standard deviation, percent change in average flight UTS as compared to the control, %E, average %E with standard deviation, and the percent change in average flight %E as compared to the control.

Table 15. Tensile Data for the MISSE-13 PCE-1 Wake Tensile Samples.

| MISSE-13 Wake ID | Flight or Control | Material | Nominal Thickness (inch) | Elastic Modulus (MPa) | Yield Strength (MPa) | UTS (MPa) | Ave. UTS (MPa) | Percent Change in UTS | % Elong. (%E) | Ave. %E | Percent Change in %E |
|---|---|---|---|---|---|---|---|---|---|---|---|
| M13W-T1 | F | FEP | 0.002 | 629.74 | 11.85 | 19.15 | 19.32 ± 0.26 | -20.1 | **165.22** | 168.91 ± 6.40 | -24.8 |
| M13W-T2 | F | | | 640.61 | 11.90 | 19.20 | | | **165.20** | | |
| M13W-T3 | F | | | 619.65 | 11.84 | 19.62 | | | **176.30** | | |
| M13W-T1 | C | FEP | 0.002 | 600.97 | 11.59 | 24.78 | 24.20 ± 1.81 | | **228** | 224.51 ± 19.84 | |
| M13W-T2 | C | | | 600.19 | 11.34 | 21.29 | | | **191.9** | | |
| M13W-T3 | C | | | 598.44 | 11.6 | 26.23 | | | **245.02** | | |
| M13W-T3.1 | C | | | 593.51 | 11.36 | 24.05 | | | **224.25** | | |
| M13W-T3.2 | C | | | 587.95 | 11.41 | 24.64 | | | **233.39** | | |
| M13W-T4 | F | FEP-AO | 0.002 | 612.40 | 11.59 | 18.70 | 17.17 ± 1.34 | -16.3 | **163.82** | 140.22 ± 20.62 | -24.8 |
| M13W-T5 | F | | | 588.41 | 11.28 | 16.21 | | | **125.64** | | |
| M13W-T6 | F | | | 597.66 | 11.30 | 16.59 | | | **131.21** | | |
| M13W-T4 | C | FEP-AO | 0.002 | 557.19 | 10.87 | 19.85 | 20.52 ± 0.55 | | **178.33** | 186.58 ± 7.43 | |
| M13W-T5 | C | | | 570.37 | 11.04 | 20.19 | | | **181.74** | | |
| M13W-T6 | C | | | 531.75 | 10.72 | 20.6 | | | **193.43** | | |
| M13W-T6.1 | C | | | 584.52 | 11.2 | 20.67 | | | **184.09** | | |
| M13W-T6.2 | C | | | 580.27 | 11.12 | 21.3 | | | **195.3** | | |
| M13W-T7 | F | C-FEP | 0.002 | 1012.62 | 11.17 | 15.44 | 17.70 ± 2.19 | -22.9 | **123.26** | 169.88 ± 42.97 | -34.5 |
| M13W-T8 | F | | | 970.77 | 11.12 | 17.85 | | | **178.46** | | |
| M13W-T9 | F | | | 1020.56 | 11.32 | 19.82 | | | **207.91** | | |
| M13W-T7 | C | C-FEP | 0.002 | 660.63 | 0.06 | 23.5 | 22.97 ± 1.72 | | **270.95** | 259.17 ± 24.20 | |
| M13W-T8 | C | | | 691.4 | 10.26 | 22.07 | | | **246.56** | | |
| M13W-T9 | C | | | 684.23 | 10.46 | 24.95 | | | **284.13** | | |
| M13W-T9.1 | C | | | 709.05 | 10.43 | 20.5 | | | **223.34** | | |
| M13W-T9.2 | C | | | 656.35 | 10.41 | 23.82 | | | **270.89** | | |
| M13W-T10 | F | FEP | 0.005 | 622.82 | 11.74 | 16.58 | 17.43 ± 1.32 | -28.5 | **155.96** | 173.75 ± 27.78 | -36.8 |
| M13W-T11 | F | | | 613.63 | 11.37 | 18.95 | | | **205.77** | | |
| M13W-T12 | F | | | 607.94 | 11.79 | 16.76 | | | **159.53** | | |
| M13W-T10 | C | FEP | 0.005 | 591.08 | 11.37 | 22.59 | 24.39 ± 1.08 | | **255.18** | 274.73 ± 12.31 | |
| M13W-T11 | C | | | 601.46 | 11.49 | 24.28 | | | **272.17** | | |
| M13W-T12 | C | | | 601.02 | 11.56 | 25.33 | | | **287.91** | | |
| M13W-T12.1 | C | | | 600.66 | 11.58 | 24.99 | | | **280.66** | | |
| M13W-T12.2 | C | | | 601.14 | 11.51 | 24.78 | | | **277.71** | | |

Table 15. Tensile Data for the MISSE-13 PCE-1 Wake Tensile Samples.

| MISSE-13 Wake ID | Flight or Control | Material | Nominal Thickness (inch) | Elastic Modulus (MPa) | Yield Strength (MPa) | UTS (MPa) | Ave. UTS (MPa) | Percent Change in UTS | % Elong. (%E) | Ave. %E | Percent Change in %E |
|---|---|---|---|---|---|---|---|---|---|---|---|
| M13W-T13 | F | FEP-AO | 0.005 | 630.50 | 11.87 | 17.33 | 19.09 ± 3.47 | -25.2 | **169.76** | 198.27 ± 54.95 | -31.4 |
| M13W-T14 | F | | | 629.56 | 11.83 | 16.85 | | | **163.43** | | |
| M13W-T15 | F | | | 621.33 | 11.73 | 23.09 | | | **261.61** | | |
| M13W-T13 | C | FEP-AO | 0.005 | 619.19 | 11.84 | 25.24 | 25.51 ± 0.28 | | **283.43** | 288.93 ± 5.22 | |
| M13W-T14 | C | | | 614.42 | 11.78 | 25.49 | | | **285.98** | | |
| M13W-T15 | C | | | 623.09 | 11.63 | 25.68 | | | **290.29** | | |
| M13W-T15.1 | C | | | 614.96 | 11.57 | 25.9 | | | **297.11** | | |
| M13W-T15.2 | C | | | 615.29 | 11.61 | 25.25 | | | **287.86** | | |
| M13W-T16 | F | C-FEP | 0.005 | 712.27 | 11.31 | 18.78 | 18.95 ± 0.50 | -15.9 | **220.06** | 221.93 ± 3.39 | -19.2 |
| M13W-T17 | F | | | 735.88 | 11.38 | 18.56 | | | **219.88** | | |
| M13W-T18 | F | | | 731.45 | 11.53 | 19.52 | | | **225.84** | | |
| M13W-T16 | C | C-FEP | 0.005 | 643.63 | 11.11 | 21.64 | 22.55 ± 1.77 | | **265.82** | 274.82 ± 23.50 | |
| M13W-T17 | C | | | 644.64 | 10.95 | 20.15 | | | **241.7** | | |
| M13W-T18 | C | | | 661.64 | 11.19 | 23.08 | | | **283.42** | | |
| M13W-T18.1 | C | | | 671.05 | 11.24 | 24.88 | | | **305.63** | | |
| M13W-T18.2 | C | | | 667.7 | 11.03 | 23 | | | **277.51** | | |
| M13W-T19 | F | VDA/CP1 | 0.0002 | 1994.01 | 80.15 | 80.15 | 94.06 ± 19.47 | -10.2 | **3.95** | 3.78 ± 0.15 | 2.5 |
| M13W-T20 | F | | | 4343.39 | 87.86 | 116.31 | | | **3.68** | | |
| M13W-T21 | F | | | 4690.52 | 49.34 | 85.71 | | | **3.72** | | |
| M13W-T19 | C | VDA/CP1 | 0.0002 | 3627.01 | 96.17 | 100.18 | 104.70 ± 3.71 | | **3.19** | 3.69 ± 0.31 | |
| M13W-T20 | C | | | 4103.68 | 88.81 | 107.76 | | | **3.61** | | |
| M13W-T21 | C | | | 3743.75 | 88.77 | 104.74 | | | **3.81** | | |
| M13W-T21.1 | C | | | 4104.44 | 85.82 | 108.89 | | | **3.92** | | |
| M13W-T21.2 | C | | | 3843.67 | 68.35 | 101.94 | | | **3.92** | | |
| M13W-T22 | F | VDA/CP1-PTFE | 0.0003 | 3323.35 | 72.12 | 92.76 | 92.25 ± 0.71 | -2.6 | **16.40** | 13.57 ± 3.17 | -4.9 |
| M13W-T23 | F | | | 3265.93 | 71.61 | 92.56 | | | **10.14** | | |
| M13W-T24 | F | | | 2927.27 | 70.99 | 91.44 | | | **14.17** | | |
| M13W-T22 | C | VDA/CP1-PTFE | 0.0003 | 3254.87 | 72.76 | 96.41 | 94.73 ± 1.95 | | **14.69** | 14.27 ± 4.26 | |
| M13W-T23 | C | | | 3655.24 | 73.35 | 96.39 | | | **9.2** | | |
| M13W-T24 | C | | | 3291.2 | 72.29 | 95.29 | | | **18.03** | | |
| M13W-T24.1 | C | | | 2975.52 | 70.6 | 91.83 | | | **18.72** | | |
| M13W-T24.2 | C | | | 3071.33 | 71.26 | 93.75 | | | **10.71** | | |

All tensile samples are cut parallel to roll lines

Figure 32 is a bar chart showing the average %E values, with standard deviation error bars, for the MISSE-13 PCE-4 Teflon FEP wake flight and control tensile samples. As stated previously, the tensile samples were all die-cut parallel to the roll direction. Once again, all of the Teflon FEP flight samples were embrittled after the 0.44 years of wake space exposure. The FEP-AO samples were flown to verify that the texturing process used to increase the adhesion of the carbon coating did not have an impact on the embrittlement of the samples. Based on the percent %E decreases as compared to control samples, the AO texturing did not cause more embrittlement as compared to the non-textured 2 mil or 5 mil FEP. The 2 mil FEP experienced a 24.8% decrease in %E, whereas the 2 mil FEP-AO also experienced a 24.8% decrease in %E. The 5 mil FEP experienced a 36.8% decrease in %E, whereas the 5 mil FEP-AO experienced a 31.4% decrease in %E.

The MISSE-13 wake C-FEP results were surprising because the carbon coated samples were not nearly as embrittled as the MISSE-9 C-FEP samples. The MISSE-9 samples did receive higher solar exposures, but it is not clear why the MISSE-13 wake C-FEP samples were not more embrittled as compared to the MISSE-13 uncoated FEP samples. The MISSE-13 wake 2 mil C-FEP was more embrittled then the 2 mil FEP with a decrease in %E of 34.5% (as compared to 24.8%). However, the 5 mil C-FEP appeared less embrittled than the 5 mil FEP with a decrease of only 19.2% as compared to 36.8% for the 5 mil FEP. It should be noted that the 5 mil C-FEP flight samples had a much larger %E standard deviation (±23.50) than the 5 mil FEP flight samples (±12.31).

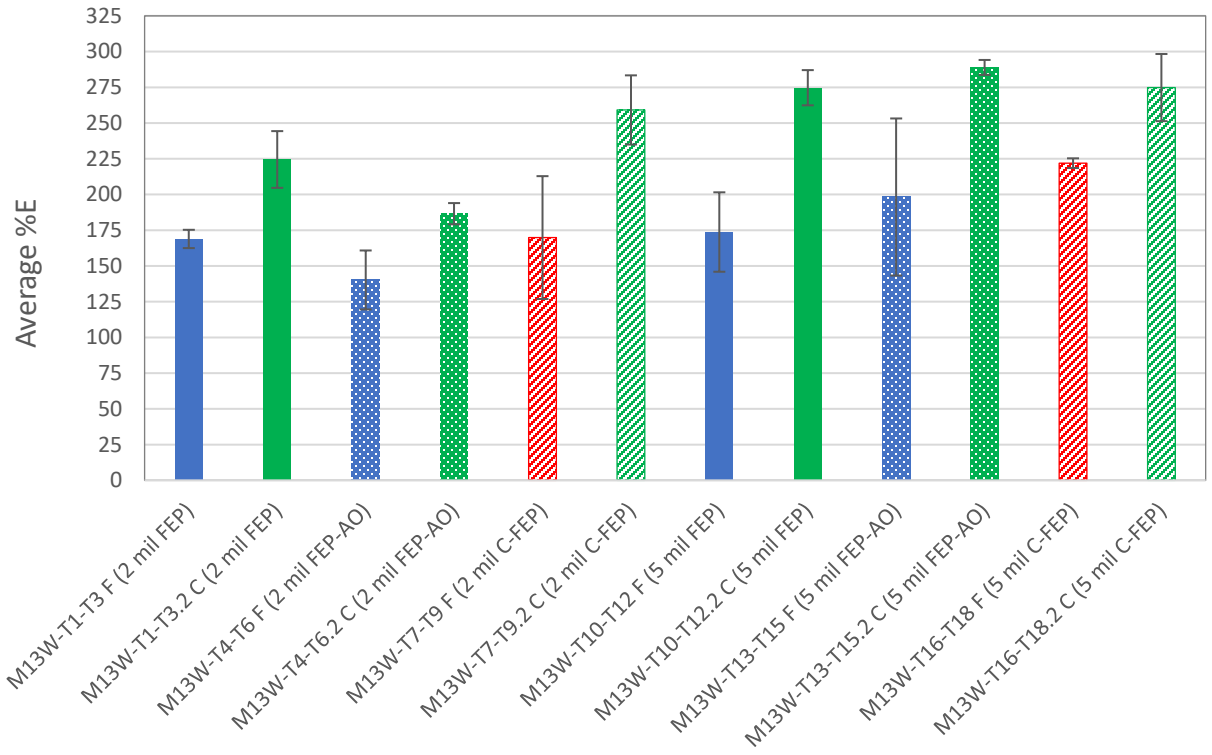


Figure 32. Bar chart showing the average %E for the MISSE-13 PCE-4 wake Teflon FEP flight (F) and control (C) samples.

Figures 33 and 34 provide stress-strain curves for the MISSE-13 PCE-4 0.2 mil VDA/CP1 and 0.3 mil VDA/CP1-PTFE wake flight and control tensile samples, respectively. It should be noted that the amount of initial slack varies widely between tests, so a toe compensation was performed as per ASTM standard D638. The toe compensation is used to calculate values for %E that more faithfully represent the material properties rather than variability in the test setup. The data is summarized in the bar chart in Figure 35, which provides the average %E values, with standard deviation error bars. The %E of the flight samples (blue) did not appear to be significantly reduced by the 0.44 year wake space exposure when compared to the control samples (green).

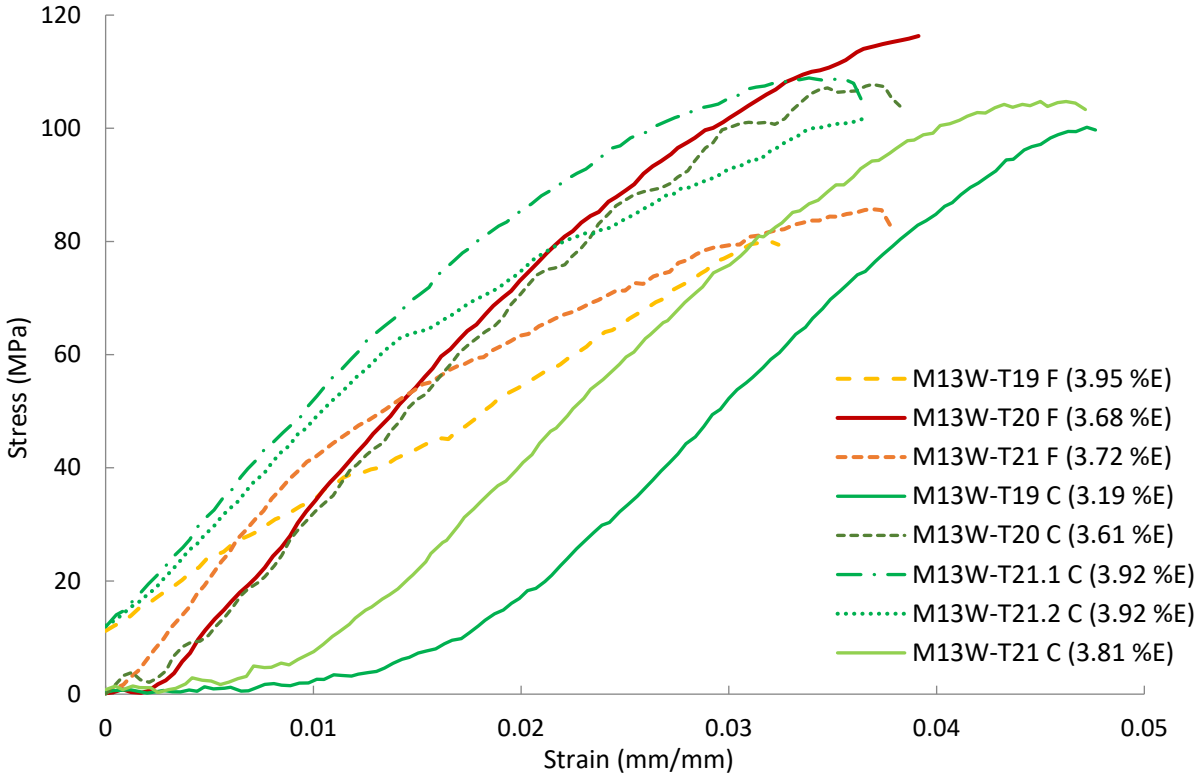


Figure 33. Stress-strain curves for the MISSE-13 PCE-4 wake 0.2 mil VDA/CP1 flight (F, yellow, orange, red) and control (C, green) samples.

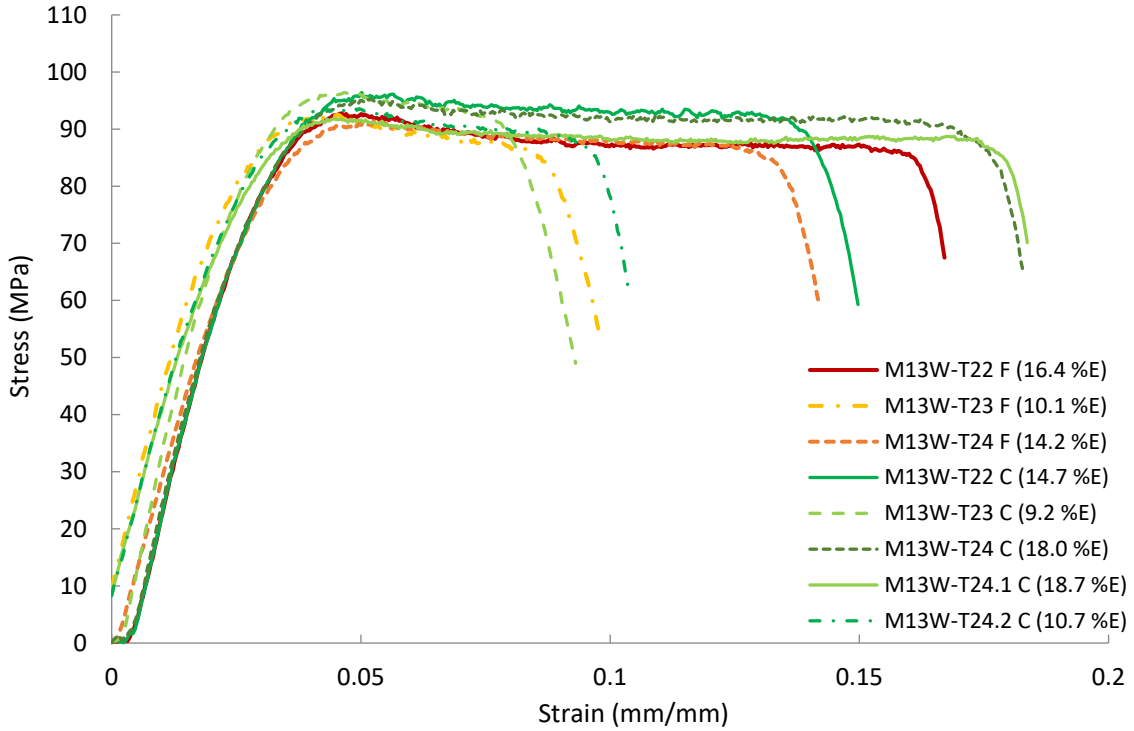


Figure 34. Stress-strain curves for the MISSE-13 PCE-4 wake 0.3 mil VDA/CP1-PTFE flight (F, yellow, orange, red) and control (C, green) samples.

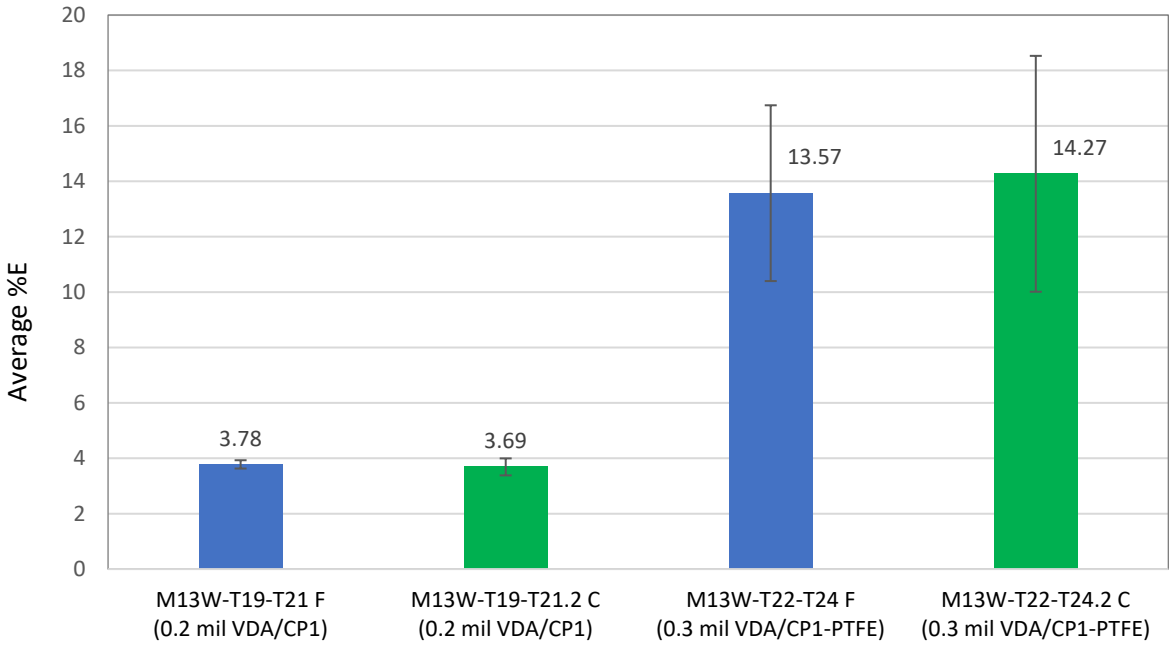


Figure 35. Bar chart showing the average %E for the MISSE-13 PCE-4 wake VDA/CP1 and VDA/CP1-PTFE flight (F, blue) and control (C, green) samples.

## Summary and Conclusions

One hundred and sixteen thin film tensile samples were exposed to the space environment on the exterior of the ISS for environmental durability assessment. The samples were flown in either zenith or wake orientations as part of three MISSE mission experiments: 1) the MISSE-8 Polymers Experiment with 30 zenith tensile samples, 2) the MISSE-9 PCE-1 with 24 zenith and 38 wake tensile samples, and 3) the MISSE-13 PCE-4 with 24 wake samples. The majority of samples were thin film Teflon FEP, a common spacecraft insulation material, with a variety of thicknesses and coatings. Two of the MISSE-9 wake samples (5 mil C-FEP) broke while on-orbit. Post-flight tensile testing was completed on 114 flight samples (30 MISSE-8 zenith, 36 MISSE-9 wake, 24 MISSE-9 zenith and 24 MISSE-13 wake) and 116 control samples (21 MISSE-8, 55 MISSE-9 and 40 MISSE-13).

All Teflon FEP samples were embrittled due to the space exposure. The zenith FEP samples were consistently more embrittled than the wake samples for the sample exposure duration (i.e. MISSE-9 zenith vs. wake). The slightly longer MISSE-9 wake exposure (0.54 years) caused more embrittlement of the Teflon FEP samples than the MISSE-13 wake exposure (0.44 years). Samples of 2 mil aluminized-Teflon FEP flown with the aluminized coating facing the space environment (Al/FEP), rather than the Teflon surface, were less embrittled than when the Teflon FEP was space facing. Thus, we can conclude that some of the damaging space radiation penetrates through 1000 Å of aluminum. The underlying layers of a multi-layered stack of 2 mil Teflon FEP were embrittled, but to a lesser extent than the top surface layer. This was consistent with prior studies that investigated the absorbed dose of radiation in Teflon FEP and indicates that deeper penetrating radiation can cause embrittlement, but less penetrating radiation appears to cause the majority of the damage. Teflon with a black carbon back-surface coating, which passively heats to a higher temperature on-orbit, was more embrittled than Al-FEP or Ag-FEP, which supports prior studies indicating that higher on-orbit temperatures cause a synergistic effect that increases the radiation-induced embrittlement of Teflon FEP in LEO. Finally, thin film solar sail materials of 0.2 mil VDA/CP1 and 0.3 mil VDA/CP1-PTFE had no significant embrittlement after 0.44 years of LEO wake exposure.

## References


1. National Aeronautics and Space Administration: U.S. Standard Atmosphere, 1976. NASA TM–X–74335, 1976.
2. Dever, J.A., “Low Earth Orbital Atomic Oxygen and Ultraviolet Radiation Effects on Polymers,” NASA TM 103711, February 1991.
3. de Groh, K.K., Banks, B.A., Miller, S.K.R., and Dever, J.A., Degradation of Spacecraft Materials (Chapter 28), Handbook of Environmental Degradation of Materials, Myer Kutz (editor), William Andrew Publishing, pp. 601–645, 2018.
4. de Groh, K. K. and McCollum, T. A., “Low Earth Orbit Durability of Protected Silicone for Refractive Photovoltaic Concentrator Arrays,” *Journal of Spacecraft and Rockets*, Vol. 32, No. 1, Jan-Feb 1995, pp. 103-109.
5. Hansen, P. A., Townsend, J. A., Yoshikawa, Y., Castro, D. J., Triolo, J. J., and Peters, W. C., SAMPE International Symposium, 43, (1998) 570.

6. Townsend, J. A., Hansen, P. A., Dever, J. A., de Groh, K. K., Banks, B. A., Wang, L., and He, C. C., "Hubble Space Telescope Metallized Teflon FEP Thermal Control Materials: On-Orbit Degradation and Post-Retrieval Analysis," *High Performance Polymers 11 (1999) 81–99.*
7. de Groh, K. K, Perry, B. A., Mohammed, J. A. and Banks, B.A., "Analyses of Hubble Space Telescope Aluminized-Teflon Multilayer Insulation Blankets Retrieved After 19 Years of Space Exposure," NASA TM-2015-218476, February 2015.
8. Yang, J. C. and de Groh, K. K., "Materials Issues in the Space Environment," MRS Bulletin, Vol. 35, January 2010, pp. 12-19.
9. de Groh, K. K. and Banks, B. A., "Space Environmental Exposure of the MISSE 9-15 Polymers and Composites Experiment 1-4 (PCE 1-4)," NASA/TM-20240000755/REV1, April 2025.
10. de Groh, K. K., Banks, B. A., Dever, J. A., Jaworske, D. J., Miller, S. K., Sechkar, E. A. and Panko, S. R., "NASA Glenn Research Center's Materials International Space Station Experiments (MISSE 1-7)," Proceedings of the International Symposium on "SM/MPAC&SEED Experiment," Tsukuba, Japan, March 10-11, 2008, JAXA-SP-08-015E, March 2009, pp. 91 – 119; also NASA TM-2008-215482, December 2008.
11. de Groh, K. K. and Banks, B. A., "Atomic Oxygen Erosion Data from the MISSE 2-8 Missions," NASA/TM-2019-219982, May 2019.
12. de Groh, K. K., Banks, B. A., McCarthy, C. E., Rucker, R. N., Roberts L. M. and Berger, L. A., "MISSE 2 PEACE Polymers Atomic Oxygen Erosion Experiment on the International Space Station," *High Performance Polymers,* 20 (2008) 388–409.
13. de Groh, K. K., Banks, B.A., Asmar, O. C., Yi, G. T., Mitchell, G. G., Guo, A. and Sechkar, E. A., "Erosion Results of the MISSE 8 Polymers Experiment After 2 Years of Space Exposure on the International Space Station," NASA TM-2017-219445, February 2017.
14. Dever, J. A., Miller, S. K., Sechkar, E. A. and Wittberg, T. N., "Space Environment Exposure of Polymer Films on the Materials International Space Station Experiment: Results from MISSE 1 and MISSE 2," *High Performance Polymers*, 20 (2008), pp. 371- 387.
15. Miller, S. K. R. and Dever, J. A., "Materials International Space Station Experiment 5 (MISSE 5) Polymer Film Thermal Control Experiment", *Journal of Spacecraft and Rockets*, Volume 48, No. 2., March-April 2011. pp 240-245.
16. Miller, S. K. R., Dever, J. A., Banks, B. A., Waters, D. L., Sechkar, E. and Kline, S., "MISSE 6 Polymer Film Tensile Experiment," Proceedings of the National Space and Missile Materials Symposium (NSMMS 2010), Scottsdale, AZ, June 28-July 1, 2010; also NASA TM-2012-217688, August 2012.
17. de Groh, K. K, Perry, B. A. and Banks, B. A., "Effect of 1.5 Years of Space Exposure on Tensile Properties of Teflon," *Journal of Spacecraft and Rockets*, Vol. 53, No. 6, November-December 2016, 1002-1011.
18. de Groh, K. K. and Banks, B. A., "MISSE-Flight Facility Polymers and Composites Experiment 1-4 (PCE 1-4)," NASA TM-20205008863, February 2021.
19. Aegis Aerospace - Commercial Space (2023): https://aegisaero.com/commercial-space-services/.
20. American Society for Testing and Materials ASTM D 638-95, "Standard Test Method for Tensile Properties of Plastics," West Conshohocken, PA, 1995.
21. Aegis Aerospace "MISSE MSC UV Equivalent Sun Hours Calculation" Report (A. Goode, MEMO-MISSE-0004 Rev C03, August 17, 2022).

22. de Groh, K. K., Lukco, D., Crowell, S. F., Gregor, S. J. and Banks, B.A., "Analyses of the MISSE 9-15 Polymers and Composites Experiment 1-4 (PCE 1-4) Contamination Samples," NASA TM-20240000941 (Corrected Copy), February 2024.
23. de Groh, K. K., Banks, B. A., Yi, G. T., Haloua, A., Imka, E. C., Mitchell, G. G., Asmar, O. C., Leneghan, H.A. and Sechkar, E. A., "Erosion Results of the MISSE 7 Polymers Experiment and Zenith Polymers Experiment After 1.5 Years of Space Exposure," NASA-TM-2016-219167 (Corrected Copy), March 2017.
24. Dever, J. A., de Groh, K. K., Banks, B. A. and Townsend, J. A., "Effects of Radiation and Thermal Cycling on Teflon FEP," *High Perform. Polym*. 11 (1999) 123-140.
25. Dever, J. A., de Groh, K. K., Banks, B. A., Townsend, J. A., Barth, J. L., Thomson, S., Gregory, T., and Savage, W., "Environmental Exposure Conditions for Teflon Fluorinated Ethylene Propylene on the Hubble Space Telescope," *High Perform. Polym*. 12 (2000) 125-139.
26. Dever, J. A. and McCracken, C. A., "Effects of Vacuum Radiation of Various Wavelengths Ranges on Teflon FEP Film, *High Perform. Polym*. 16 (2004) 289-301.
27. de Groh, K. K., Banks, B. A., Sechkar, E. A. and Scheiman, D. A., "Simulated Solar Flare X-Ray and Thermal Cycling Durability Evaluation of Hubble Space Telescope Thermal Control Candidate Replacement Materials," Presented at the 4th ICPMSE Conference, Toronto, Canada, April 23-24, 1998; NASA TM-1998-207426, December 1998.
28. de Groh, K. K. and Gummow, J. D., "Effect of Air and Vacuum Storage on the Tensile Properties of X-ray Exposed Aluminized-FEP," *High Perform. Polym*. 13, (2001) S421-S431.
29. de Groh, K. K. and Martin, M., "Thermal Contributions to the Degradation of Ground-Laboratory and Space-Irradiation Teflon®," *Journal of Spacecraft and Rockets*, Vol. 41, No. 3, May-June 2004, 366-372.

# Appendix—Manufacturer Information

Table A-1. MISSE-8 Zenith Tensile Samples Manufacturer Information.

| GRC Sample ID | Sample | Abbrev. | Thickness (mil) | Manufacturer and Lot # |
|---|---|---|---|---|
| M8-6<br>M8-11 | Teflon FEP | FEP | 2 | "Round Robin" FEP<br>DuPont #41458 |
| M8-7 | Aluminized-Teflon FEP | Al-FEP | 2 | Sheldahl<br>#502532-2 |
| M8-8 | Carbon back-surface coated FEP* | FEP/C | 2 | DuPont<br>#41458 |
| M8-9 | CP1 Polyimide | CP1 | 1.07 | SRS Technologies<br>#4648321-003 |

*Carbon back-surface coated at NASA Glenn Research Center

Table A-2. MISSE-9 Wake and Zenith Tensile Samples Manufacturer Information.

| MISSE-9 ID | Material | Abbreviation | Thickness (mils) | Manufacturer and Lot # |
|---|---|---|---|---|
| M9W-T1 to T5<br>M9W-T6 to T10<br>M9W-T35 to T38<br>M9Z-T1 to T4<br>M9Z-T5 to T8<br>M9Z-T21 to T24 | Aluminized-Teflon FEP | Al-FEP | 2 | Sheldahl<br>#502532-2 |
| M9W-T11 to T15<br>M9W-T16 to T20<br>M9Z-T9 to T12<br>M9Z-T13 to T16 | Aluminized-Teflon FEP | Al-FEP | 5 | Sheldahl<br>#502303 |
| M9W-T21 to T24 | Silver-Teflon<br>(FEP/Ag/Inconel) | Ag-FEP | 5 | Sheldahl<br>#140534 |
| M9W-T25 to T29<br>M9W-T30 to T24<br>M9Z-T17 to T20 | Back-surface carbon painted<br>(India Ink) Teflon-FEP* | C-FEP | 2 | "Round Robin" FEP<br>DuPont #41458 |

*Carbon painted (India Ink) at NASA Glenn Research Center

Table A-3. MISSE-13 Wake Tensile Samples Manufacturer Information.

| MISSE-13 ID | Material | Abbreviation | Thickness (mils) | Manufacturer and Lot # |
|---|---|---|---|---|
| M13W-T1 to T3<br>M13W-T4 to T6*<br>M13W-T7 to T9** | Teflon FEP | FEP<br>FEP-AO*<br>FEP/C** | 2 | Sheldahl<br>#96-04 |
| M13W-T10 to T12<br>M13W-T13 to T15*<br>M13W-T16 to T18** | Teflon FEP | FEP<br>FEP-AO*<br>FEP/C** | 5 | Sheldahl<br>#96-16 |
| M13W-T19 to T21 | VDA/CP1 solar sail material<br>(CP1: Polyimide Colorless) | VDA/CP1 | 0.2 | NeXolve<br>DLR10p73A |
| M13W-T22 to T24 | VDA/CP1-PTFE composite solar<br>sail material | VDA/CP1-<br>PTFE | 0.3 | NeXolve<br>DLR10p71A |

*AO textured on back surface at NASA Glenn Research Center
**AO textured and C coated on the back surface at NASA Glenn Research Center